CHAPTER 8 CONCLUSIONS & FUTURE WORK

This thesis has reached the following conclusions:

1) *Under most irradiation conditions, chromium enriches at grain boundaries in F-M alloys, and this observation can be explained by differences in solute-defect diffusion rates*. Consistent Cr enrichment has been observed in all four alloys studied in this work--T91, HCM12A, HT9, and a 9Cr model alloy—over a wide temperature range of 300-600°C, at doses of up to 10 dpa. Only one instance of Cr depletion has been observed, in T91 irradiated to 3 dpa at 700°C. Chromium RIS in F-M alloys occurs in small amounts; no more than 2.5 wt% Cr enrichment was ever recorded. These behaviors are in quite stark contrast to Cr RIS tendencies in austenitic steels, in which Cr depletion of up to 20 wt% has been routinely measured.

The inverse Kirkendall mechanism can explain the observed differences in Cr RIS between F-M and austenitic alloys. In austenitic alloys, the diffusion coefficient ratio of Cr to Ni for vacancies is greater than unity, while that for interstitials is less than unity, particularly in the temperature range of interest. The relative magnitude of these ratios mean that RIS in austenitic steels should be dominated by Cr transport via vacancies, resulting in Cr depletion. In addition, because the difference between the vacancy and interstitial diffusion coefficients is rather large, the expected amount of RIS will also be large.

However, in F-M alloys, the diffusion coefficient ratios of Cr to Fe for vacancies and for interstitials are both greater than unity and are of almost identical magnitudes. This means that both vacancies and interstitials are causing Cr RIS, the vacancies causing depletion and the interstitials, enrichment. At any particular temperature, whichever diffusion coefficient ratio—that for vacancies, or that for interstitials—is greater will decide the direction of RIS. In most of the conditions studied in this thesis, the interstitial diffusion coefficient was greater than that for vacancies, causing the observed Cr enrichment. And since the vacancy and interstitial diffusion coefficients are similar in magnitude, the difference between them is small, so the expected amount of RIS will also be small.

2) *A "crossover" from Cr enrichment to Cr depletion occurs between 600°C and 700°C in alloy T91, and this provides further confirmation for the inverse Kirkendall mechanism of Cr RIS in F-M alloys*. In alloy T91 irradiated to 3 dpa, Cr enrichment is observed at 600°C, and Cr depletion at 700°C. The temperature interval in which the crossover occurs is consistent with the crossover predicted by the diffusion coefficient ratios of Cr to Fe for vacancies and for interstitials. As mentioned in the preceding paragraph, the diffusion coefficient ratios in F-M alloys are similar in magnitude. But small differences in their slopes cause the vacancy and interstitial diffusion coefficient ratios to cross one another near ~660°C. At temperatures below the crossover temperature, the diffusion coefficient ratio for interstitials exceeds that for vacancies, which can explain the observed Cr enrichment in T91 irradiated between 300°C and 600°C. But above the crossover temperature, the diffusion coefficient ratio for vacancies becomes greater than that for interstitials, which explains the observed Cr depletion in T91 at 700°C. The existence of a crossover behavior is particular to the F-M alloy system. The existence of a crossover between Cr enrichment and Cr depletion in F-M alloys provides support for the inverse Kirkenall mechanism.

3) *The amount of Cr enrichment decreases with increasing bulk Cr concentration, and this behavior can also be attributed to differences in diffusion rates between atomic species*. Chromium enrichment is measured in T91, HCM12A, HT9, and the 9Cr model alloy following 3 dpa irradiation at 400°C. The amount of Cr enrichment is observed to decrease as a function of increasing bulk Cr concentration. The inverse Kirkendall model calculates a consistent behavior, as long as Cr-composition-dependent interstitial migration energies for both Fe and Cr are input into the model. Composition-dependent interstitial migration energies are calculated for bulk Cr concentrations less than or greater than 9 wt% Cr; the migration energies for 9 wt% Cr are fixed at their original values.

The decreasing amount of Cr with increasing bulk Cr concentration, as measured in the 400°C experiment, can be explained by differences in atomic diffusion rates. When composition-dependent interstitial migration energies are used for alloys with bulk Cr concentration > 9 wt%, the diffusion coefficient ratio of Cr to Fe for interstitials decreases slightly in magnitude, causing two major effects. First, the predicted crossover temperature decreases, although Cr is still calculated to enrich at the experiment temperature of 400°C. Second, the Cr-to-Fe interstitial diffusion coefficient ratio moves closer to that of vacancies at 400°C. The difference between the two diffusion coefficient ratio lines becomes even smaller, and thus, the expected amount of Cr RIS should be even smaller than at lower bulk Cr concentrations.

4) *The experimentally observed Cr RIS behaviors cannot be attributed to the solute drag mechanism*. When the solute drag mechanism is incorporated into the IK model using a positive Cr-interstitial binding energy, unreasonably large amounts of Cr enrichment are calculated. Conversely, when the solute drag mechanism implements a positive Cr-vacancy binding energy, unreasonable quantities of Cr depletion are calculated. Clearly, the solute drag mechanism results in Cr RIS that is entirely inconsistent with experimental measurements

6) *The behavior of Cr RIS—and thus, of Fe RIS, as well—in F-M alloys is largely consistent with the inverse Kirkendall mechanism and not consistent with the solute drag mechanism, supporting IK as the mechanism controlling Cr RIS in commercial F-M alloys.*

7) *Minor elements such as Si, Ni, and Cu, segregate by a different, yet undetermined mechanism, than that by which Cr and Fe segregate*. RIS of minor elements exhibit a different temperature dependence than does RIS of Cr and Fe. The temperature range over which the minor elements segregate is more limited (400-500°C) than that over which Cr and Fe segregate (at least 300-700°C). However, the driving mechanism of minor element RIS has not been determined.

While some notable conclusions have been reached in this work, there remain some unanswered questions that deserve future attention:

1) *There remain unresolved issues with the dose dependence of Cr RIS, especially with respect to the interrelationship of RIS and microstructure*. There are

significant differences in the kinetics of RIS between the IK model and experiment, particularly regarding the onset of RIS and the onset of steady-state RIS. It is theorized that the model-experiment difference in the onset dose may be due to a microstructurally-related incubation period in the experimental steels. It is also theorized that the model-experiment difference in the steady-state RIS behavior is due to microstructural evolution. Future work could more closely study the microstructural issues and kinetics of RIS in the IK mechanism. In addition, studying RIS at the boundaries of microstructural features such as dislocation loops and precipitates, may offer further insight into the RIS-microstructure relationship.

2) *The RIS mechanism of minor elements in F-M alloys has yet to be determined*. Work in this thesis, particularly in the modeling effort, has focused largely on Cr and Fe RIS. However, it has been concluded that minor elements Si, Ni, and Cu segregate by a different mechanism than that by which Cr and Fe segregate. This conclusion necessitates further study into the mechanism driving RIS of the minor elements. Furthermore, only a limited number of minor elements have been studied in this thesis, due to detectability issues with the STEM technique. Future work should use a technique capable of detecting a greater number of the constituent elements, in order to determine whether additional elements are segregating.

APPENDIX A: Temperature Histograms

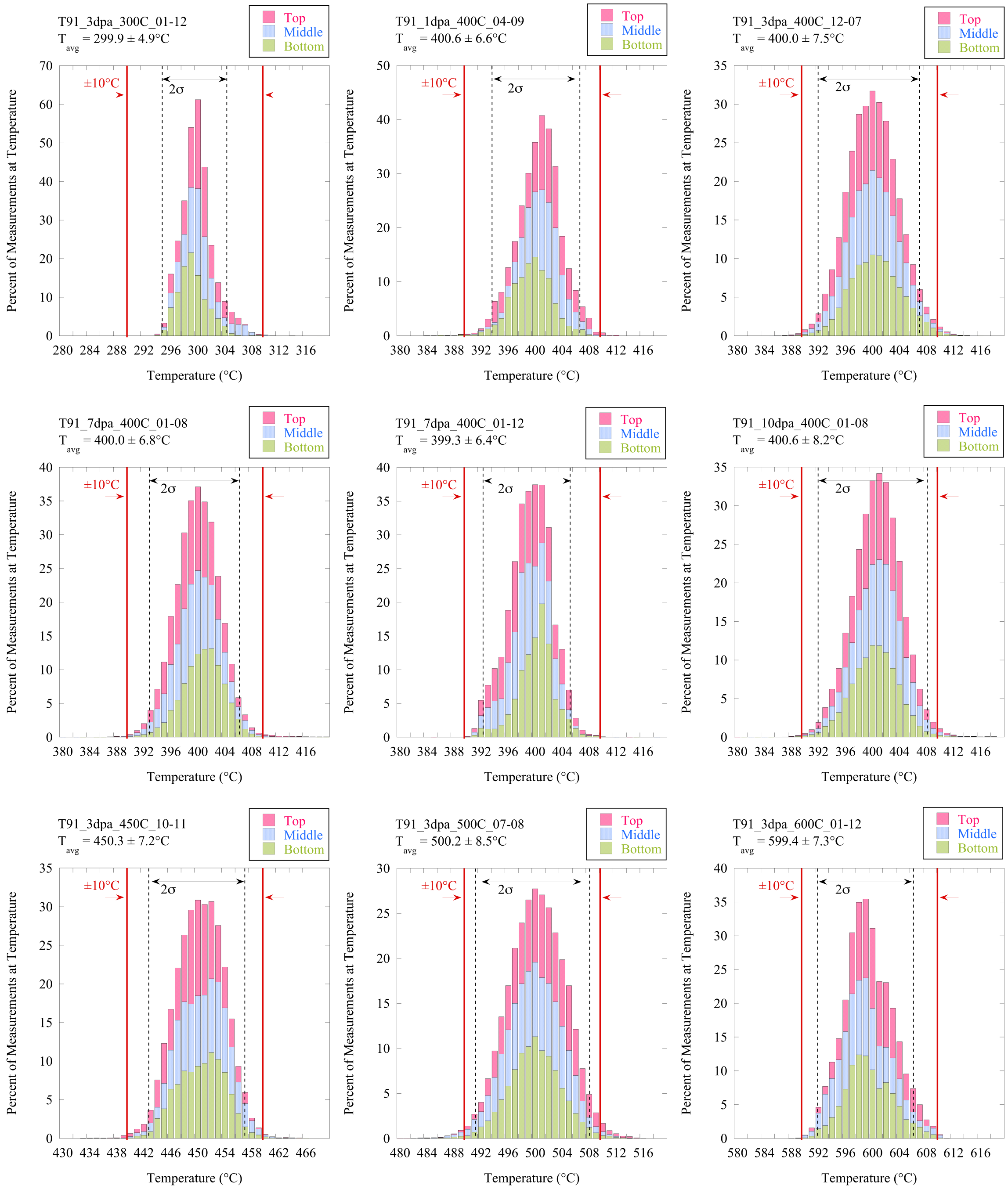
T91_3dpa_300C_01-12
T_{avg} = 299.9 ± 4.9°C
T91_1dpa_400C_04-09
T_{avg} = 400.6 ± 6.6°C
T91_3dpa_400C_12-07
T_{avg} = 400.0 ± 7.5°C
T91_7dpa_400C_01-08
T_{avg} = 400.0 ± 6.8°C
T91_7dpa_400C_01-12
T_{avg} = 399.3 ± 6.4°C
T91_10dpa_400C_01-08
T_{avg} = 400.6 ± 8.2°C
T91_3dpa_450C_10-11
T_{avg} = 450.3 ± 7.2°C
T91_3dpa_500C_07-08
T_{avg} = 500.2 ± 8.5°C
T91_3dpa_600C_01-12
T_{avg} = 599.4 ± 7.3°C
Top
Middle
Bottom
±10°C
2σ
Percent of Measurements at Temperature
Temperature (°C)

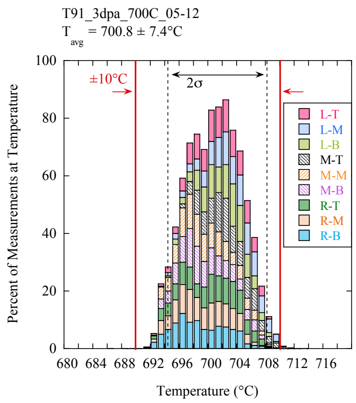
T91_3dpa_700C_05-12
T avg = 700.8 ± 7.4°C
±10°C
2σ
L-T
L-M
L-B
M-T
M-M
M-B
R-T
R-M
R-B
Percent of Measurements at Temperature
Temperature (°C)

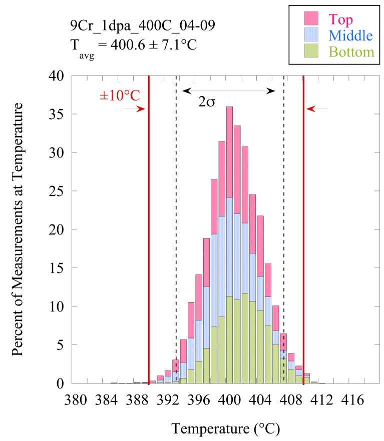
9Cr_1dpa_400C_04-09
T avg = 400.6 ± 7.1°C
Top
Middle
Bottom
±10°C
2σ
Percent of Measurements at Temperature
Temperature (°C)

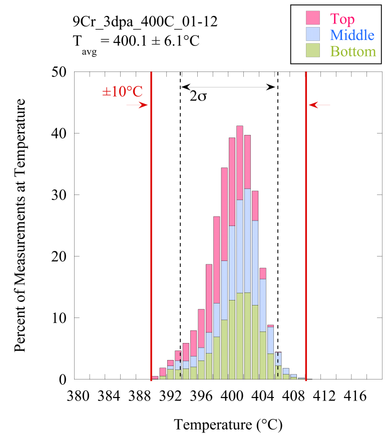
9Cr_3dpa_400C_01-12
T avg = 400.1 ± 6.1°C
Top
Middle
Bottom
±10°C
2σ
Percent of Measurements at Temperature
Temperature (°C)

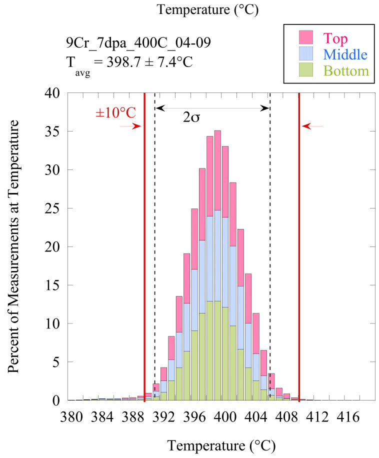
9Cr_7dpa_400C_04-09
T avg = 398.7 ± 7.4°C
Top
Middle
Bottom
±10°C
2σ
Percent of Measurements at Temperature
Temperature (°C)

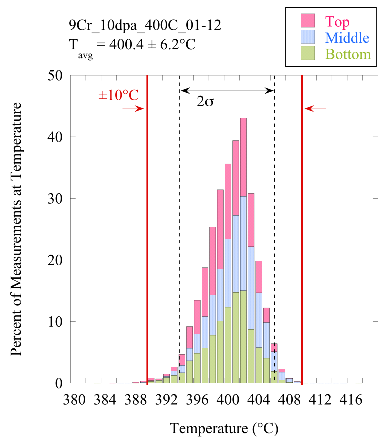
9Cr_10dpa_400C_01-12
T avg = 400.4 ± 6.2°C
Top
Middle
Bottom
±10°C
2σ
Percent of Measurements at Temperature
Temperature (°C)

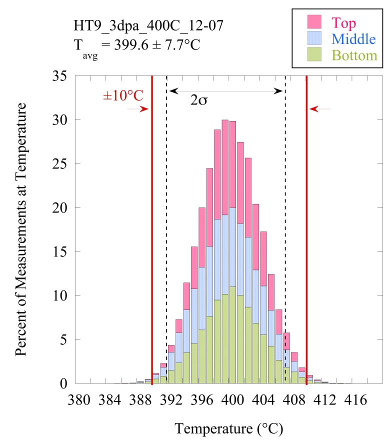
HT9_3dpa_400C_12-07
T avg = 399.6 ± 7.7°C
Top
Middle
Bottom
±10°C
2σ
Percent of Measurements at Temperature
Temperature (°C)

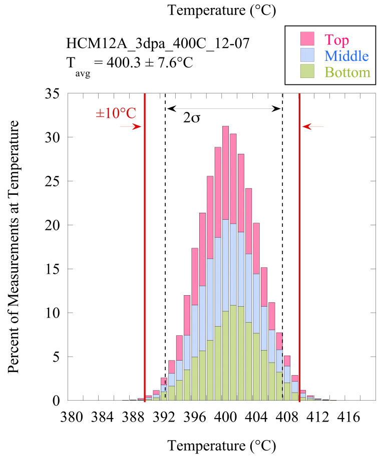
HCM12A_3dpa_400C_12-07
T avg = 400.3 ± 7.6°C
Top
Middle
Bottom
±10°C
2σ
Percent of Measurements at Temperature
Temperature (°C)

APPENDIX B: Composition Profiles

T91_UI

T91_UI_1-1-F

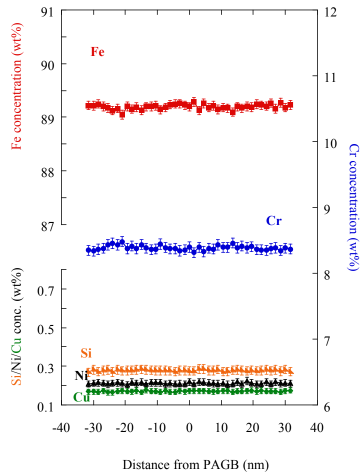

T91_UI_1-2-F

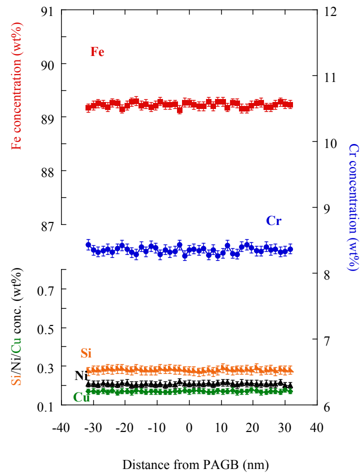

T91_UI_1-3-F

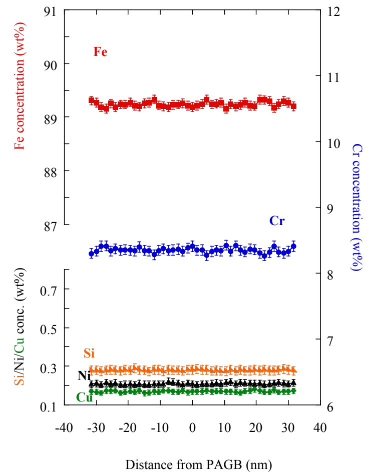

T91_UI_2-1-F

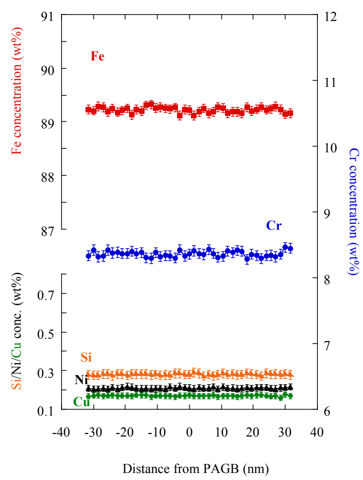

T91_UI_2-2-F

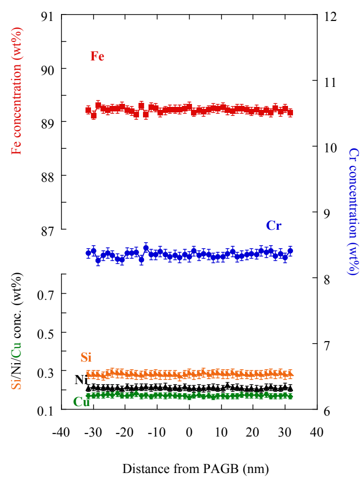

T91_UI_2-3-F

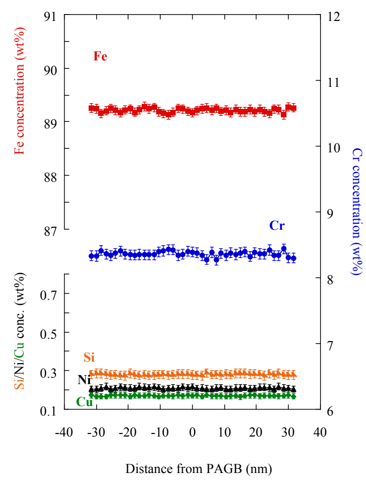

T91_UI_3-1-F

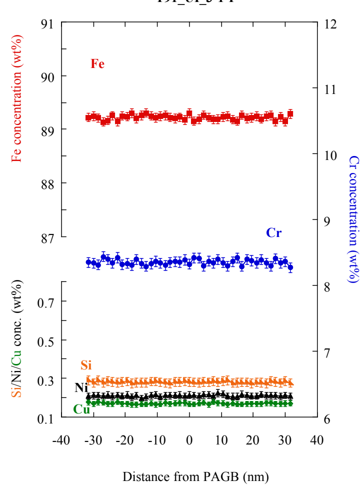

T91_UI_3-2-F

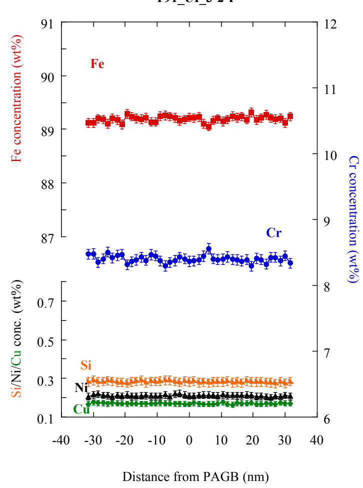

T91_UI_3-3-F

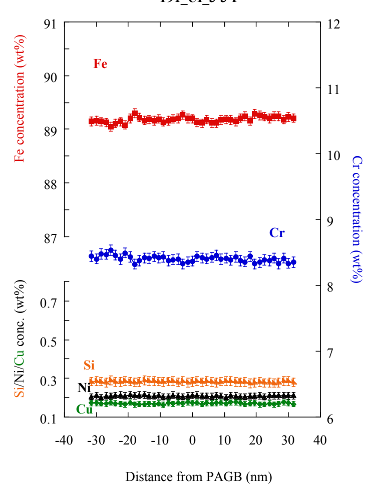

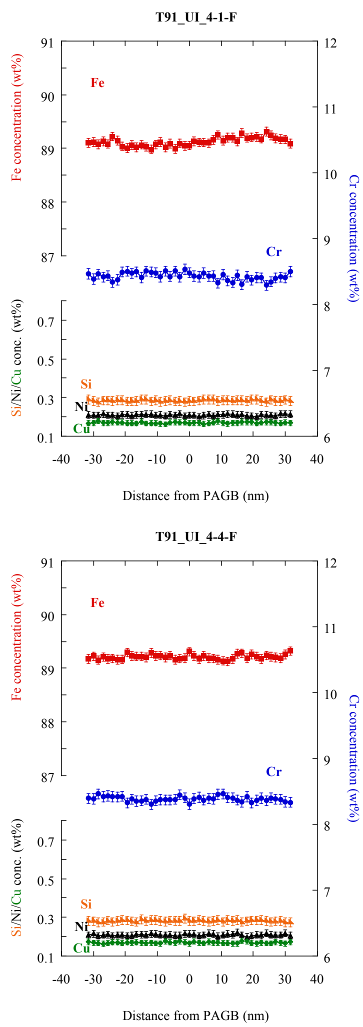
T91_UI_4-1-F
T91_UI_4-2-F
T91_UI_4-3-F
T91_UI_4-4-F
Fe
Cr
Si
Ni
Cu
Fe concentration (wt%)
Cr concentration (wt%)
Si/Ni/Cu conc. (wt%)
Distance from PAGB (nm)

9Cr_UI

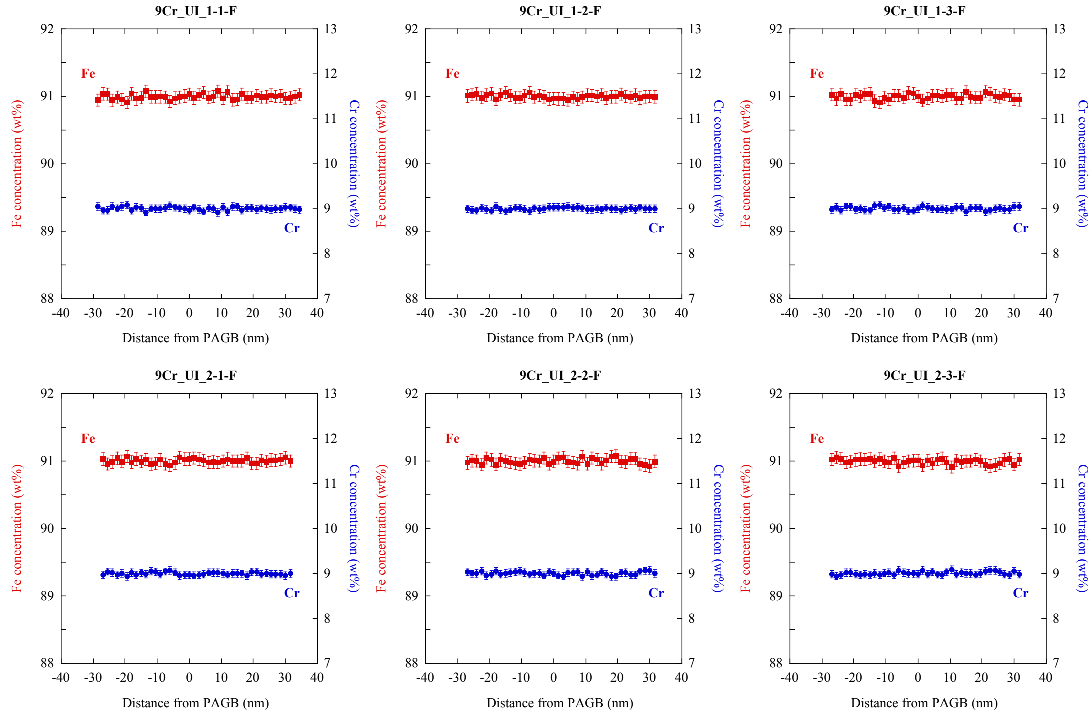
9Cr_UI_1-1-F
9Cr_UI_1-2-F
9Cr_UI_1-3-F
9Cr_UI_2-1-F
9Cr_UI_2-2-F
9Cr_UI_2-3-F
Fe
Cr
Fe concentration (wt%)
Cr concentration (wt%)
Distance from PAGB (nm)

HT9_UI

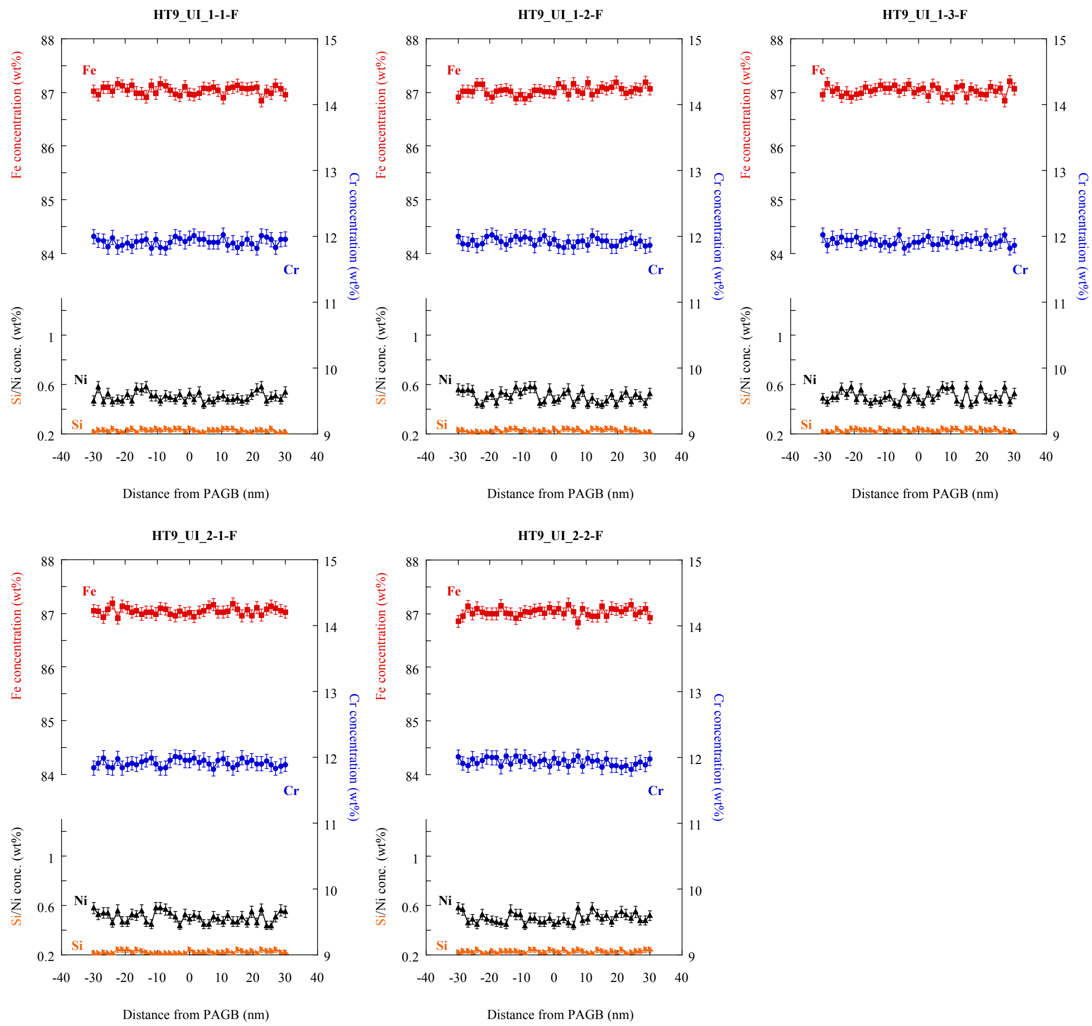
HT9_UI_1-1-F
HT9_UI_1-2-F
HT9_UI_1-3-F
HT9_UI_2-1-F
HT9_UI_2-2-F
Fe
Cr
Ni
Si
Fe concentration (wt%)
Cr concentration (wt%)
Si/Ni conc. (wt%)
Distance from PAGB (nm)

HCM12A_UI

HCM12A_UI_1-1-F

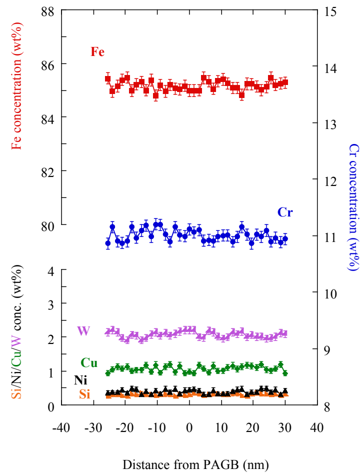

HCM12A_UI_1-2-F

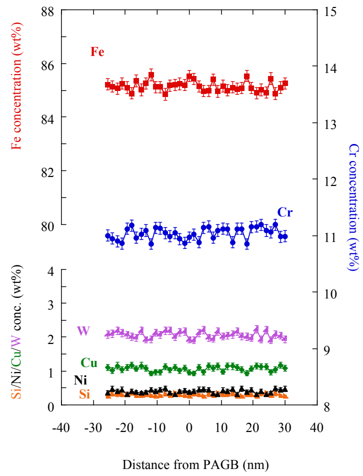

HCM12A_UI_1-3-F

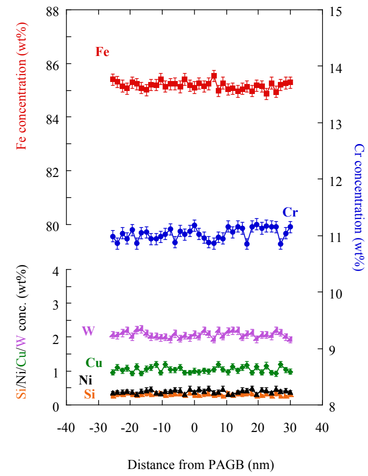

HCM12A_UI_2-1-F

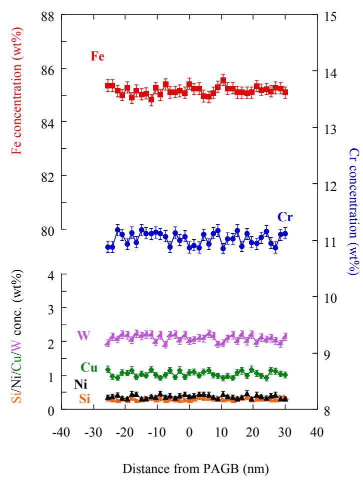

HCM12A_UI_2-2-F

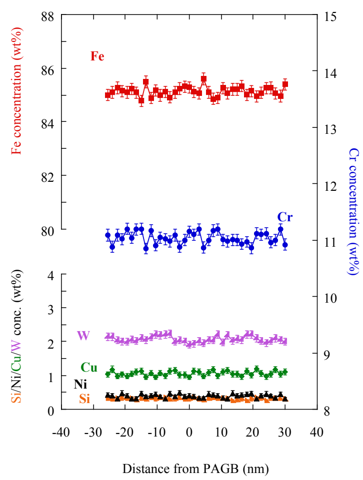

HCM12A_UI_2-3-F

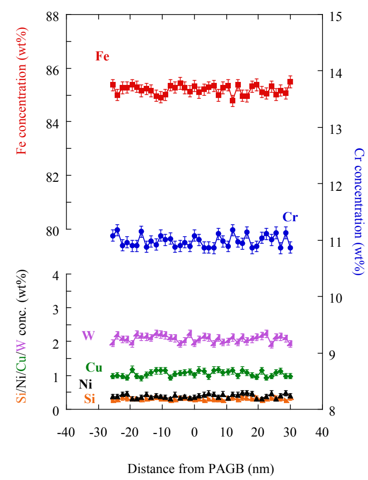

HCM12A_UI_3-1-F

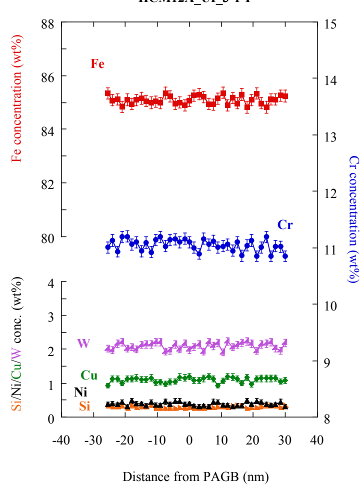

HCM12A_UI_3-2-F

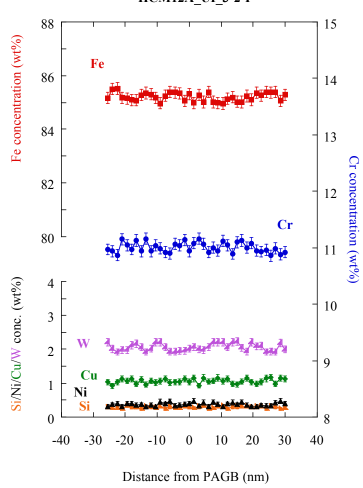

HCM12A_UI_3-3-F

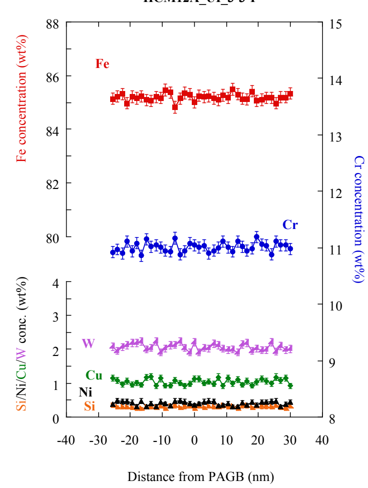

T91_3dpa_300C_01-12

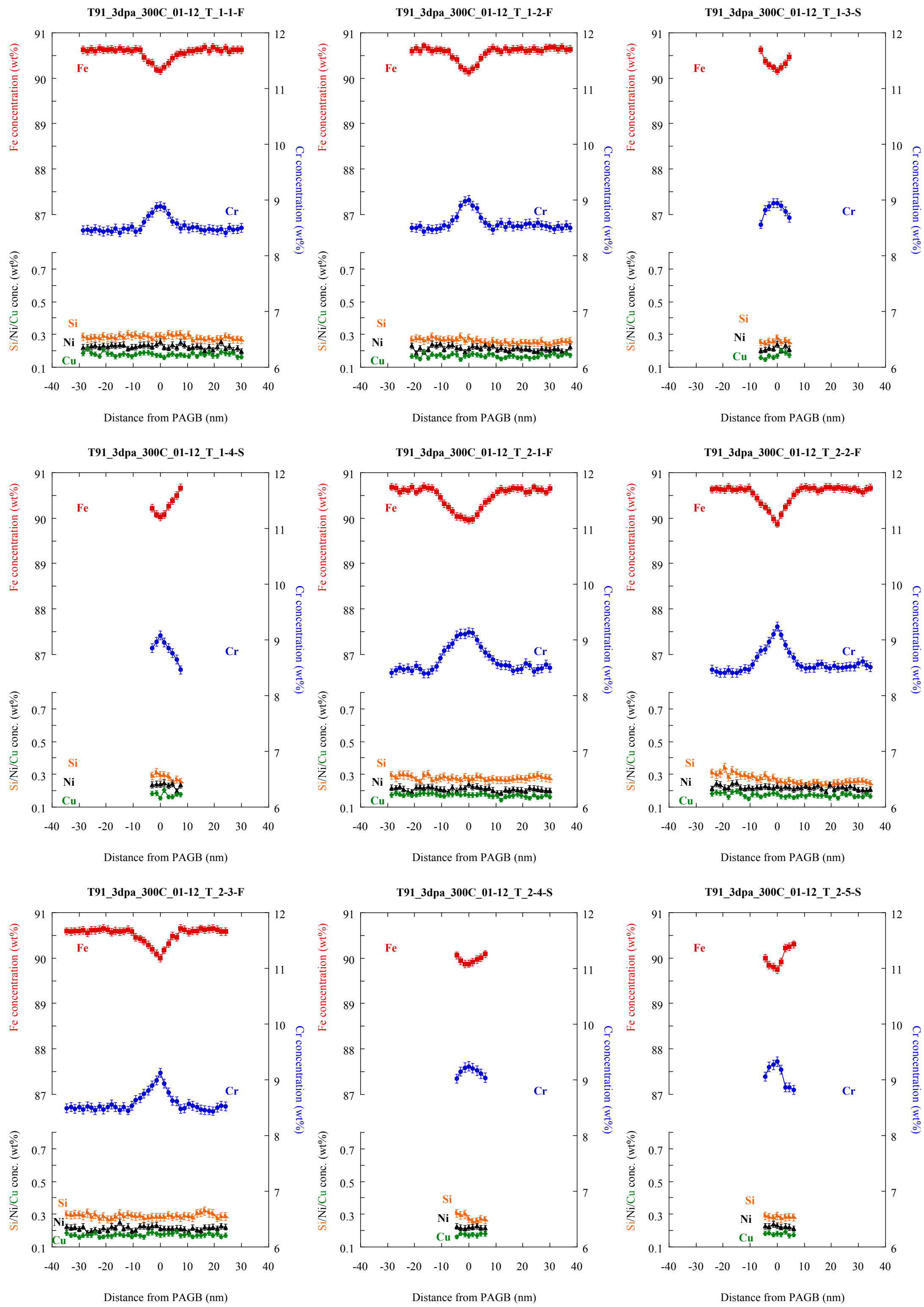

T91_1dpa_400C_04-09

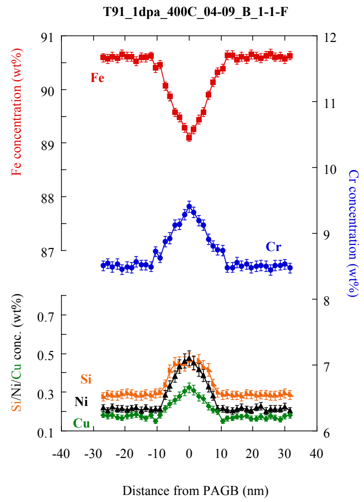

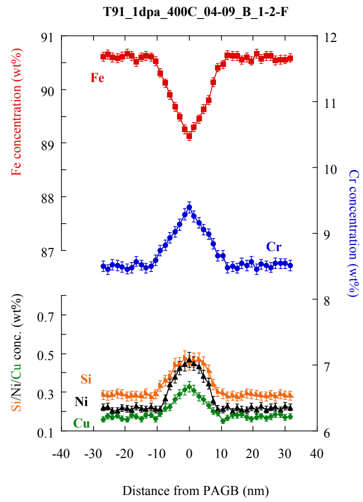

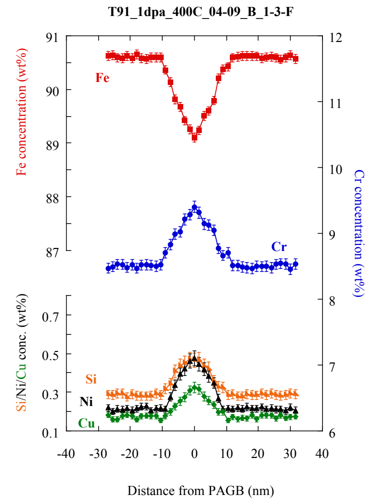

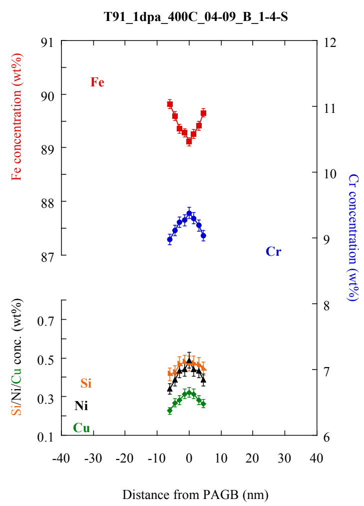

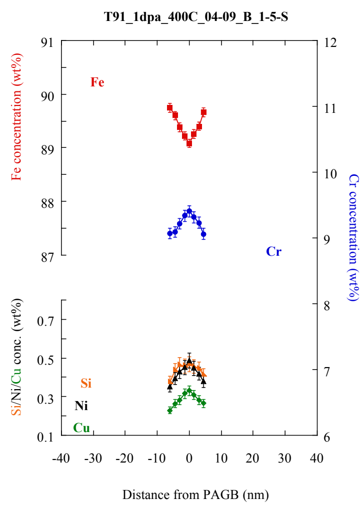

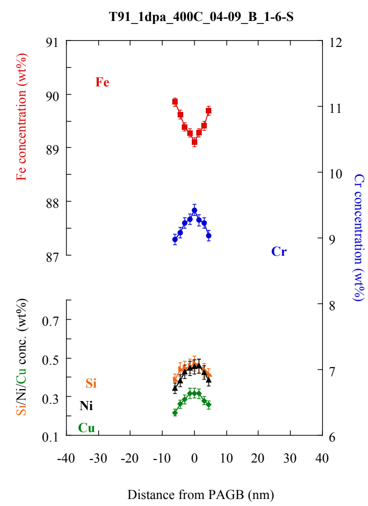

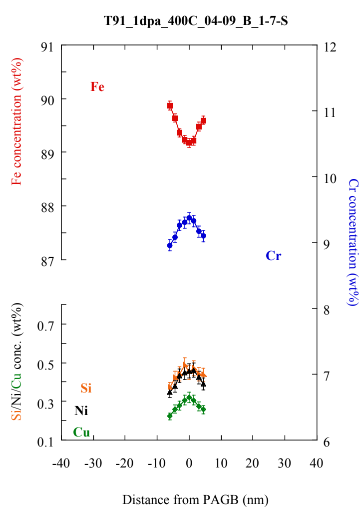

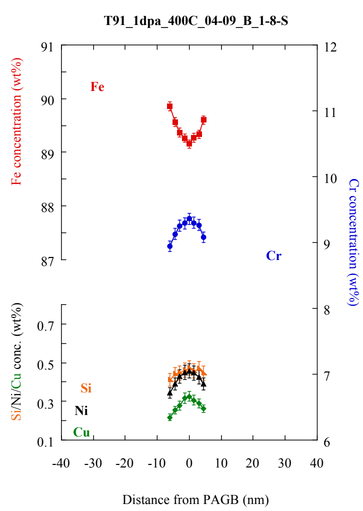

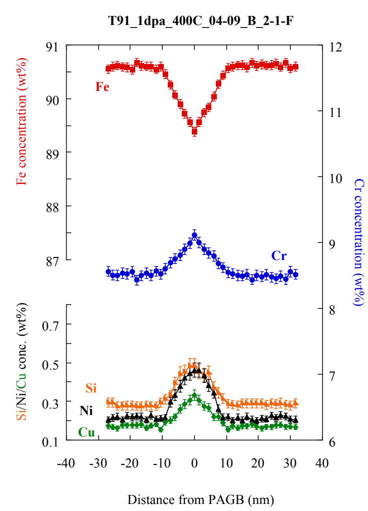

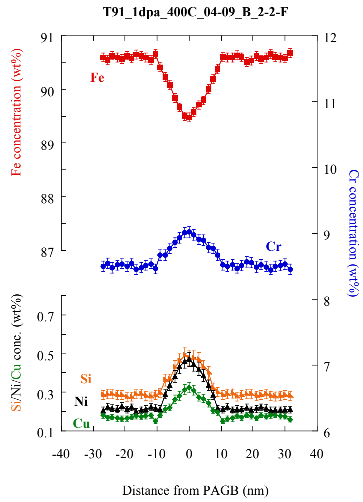
T91_1dpa_400C_04-09_B_2-2-F
Fe
Cr
Si
Ni
Cu
Fe concentration (wt%)
Cr concentration (wt%)
Si/Ni/Cu conc. (wt%)
Distance from PAGB (nm)

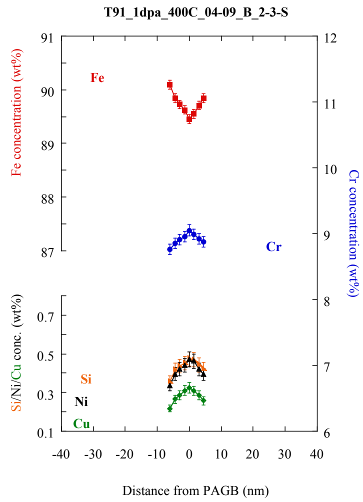
T91_1dpa_400C_04-09_B_2-3-S
Fe
Cr
Si
Ni
Cu
Fe concentration (wt%)
Cr concentration (wt%)
Si/Ni/Cu conc. (wt%)
Distance from PAGB (nm)

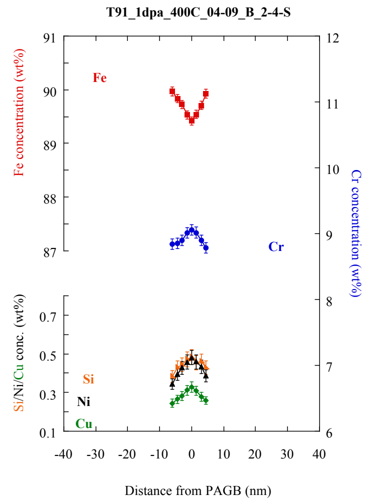
T91_1dpa_400C_04-09_B_2-4-S
Fe
Cr
Si
Ni
Cu
Fe concentration (wt%)
Cr concentration (wt%)
Si/Ni/Cu conc. (wt%)
Distance from PAGB (nm)

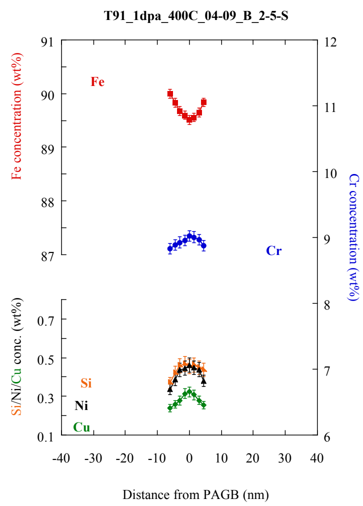
T91_1dpa_400C_04-09_B_2-5-S
Fe
Cr
Si
Ni
Cu
Fe concentration (wt%)
Cr concentration (wt%)
Si/Ni/Cu conc. (wt%)
Distance from PAGB (nm)

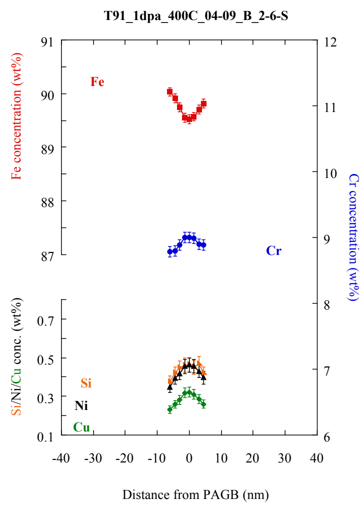
T91_1dpa_400C_04-09_B_2-6-S
Fe
Cr
Si
Ni
Cu
Fe concentration (wt%)
Cr concentration (wt%)
Si/Ni/Cu conc. (wt%)
Distance from PAGB (nm)

T91_3dpa_400C_12-07

T91_3dpa_400C_12-07_M_1-1-F

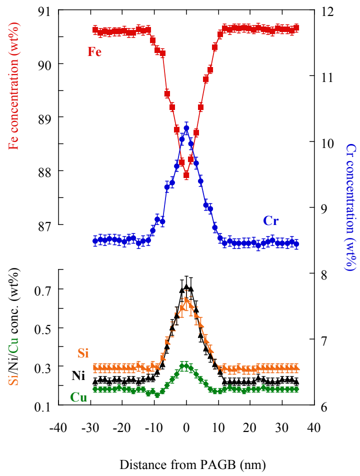

T91_3dpa_400C_12-07_M_1-2-F

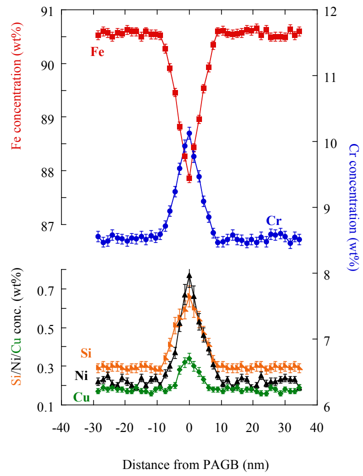

T91_3dpa_400C_12-07_M_2-1-F

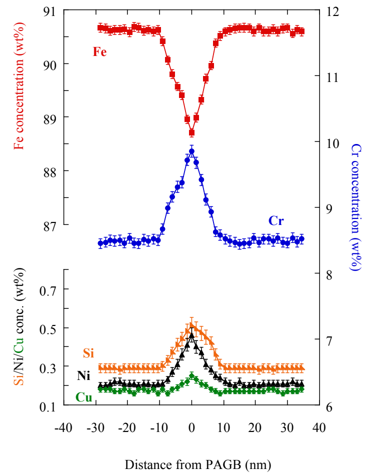

T91_3dpa_400C_12-07_M_2-2-F

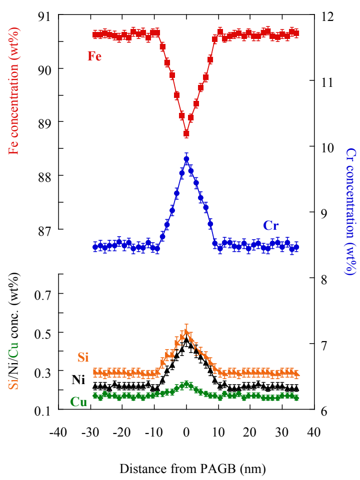

T91_3dpa_400C_12-07_M_2-3-F

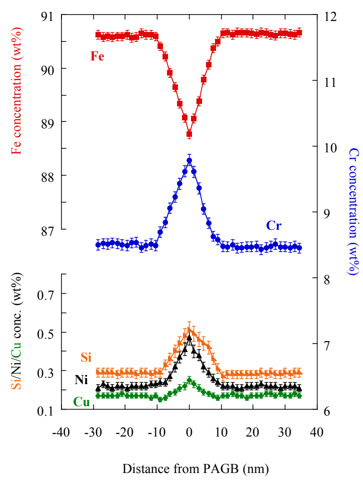

T91_3dpa_400C_12-07_M_3-1-F

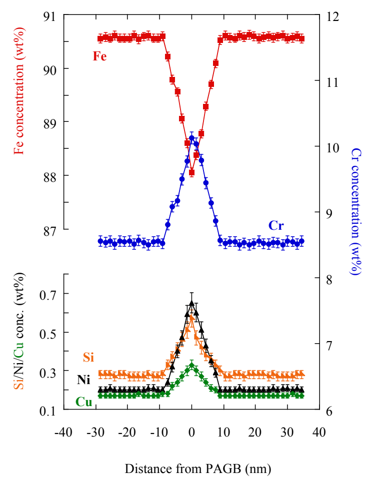

T91_3dpa_400C_12-07_M_3-2-F

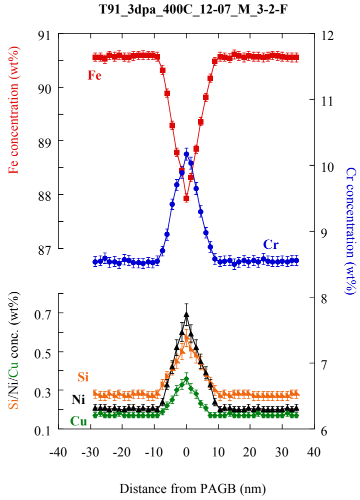

T91_7dpa_400C_01-08

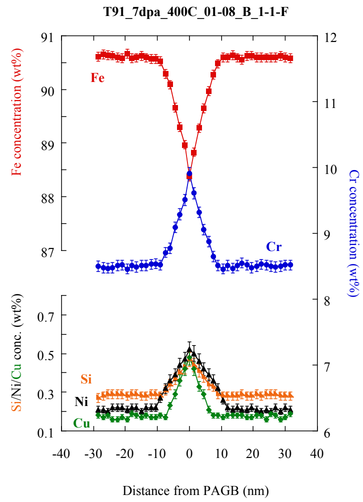

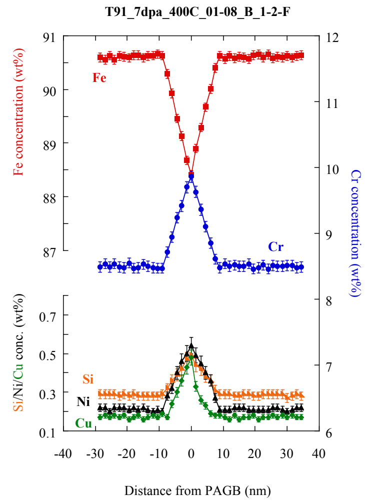

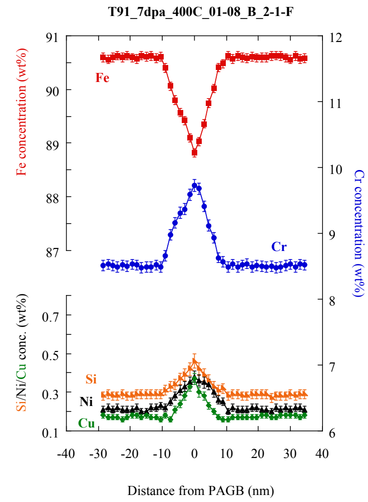

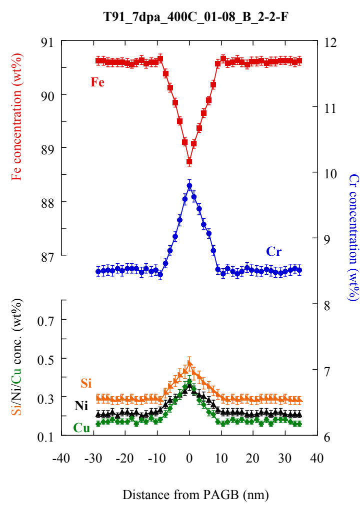

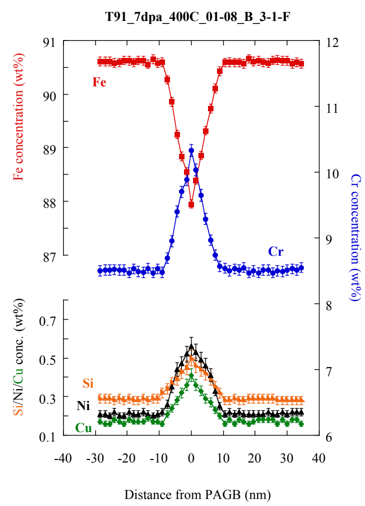

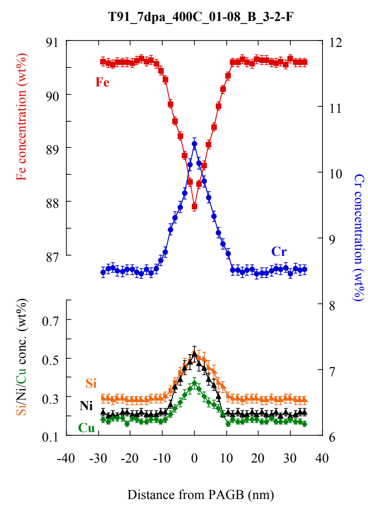

T91_7dpa_400C_01-12

T91_7dpa_400C_01-12_M_1-1-F

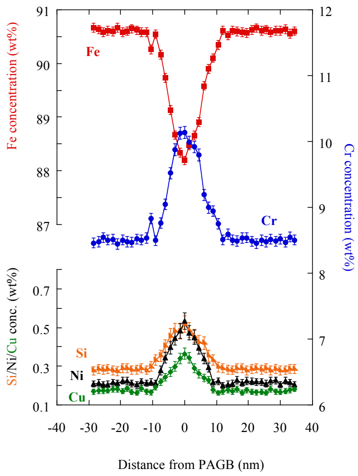

T91_7dpa_400C_01-12_M_1-2-F

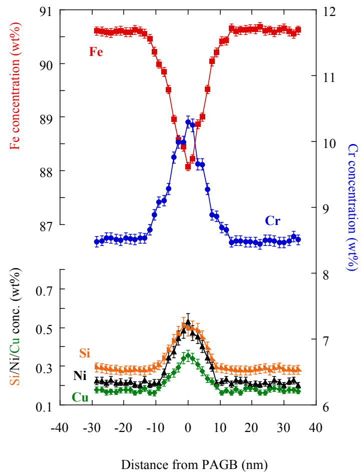

T91_7dpa_400C_01-12_M_1-3-F

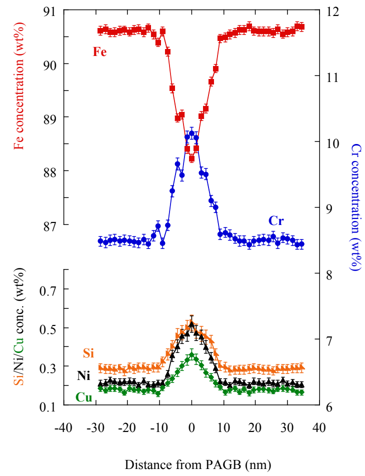

T91_7dpa_400C_01-12_M_1-4-F

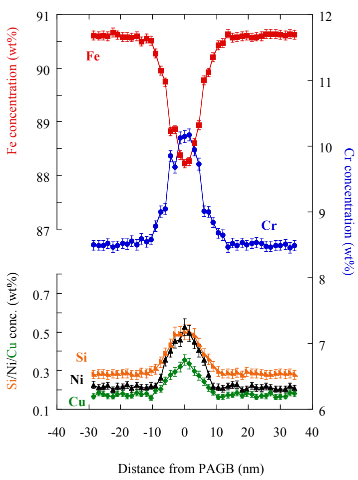

T91_7dpa_400C_01-12_M_1-5-F

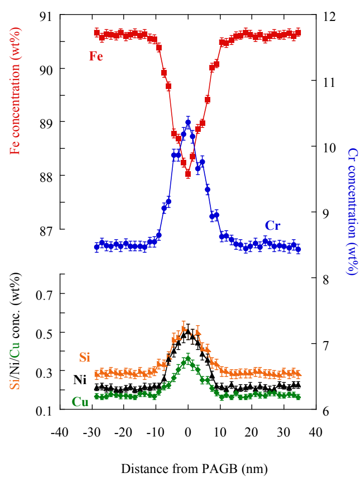

T91_7dpa_400C_01-12_M_1-6-F

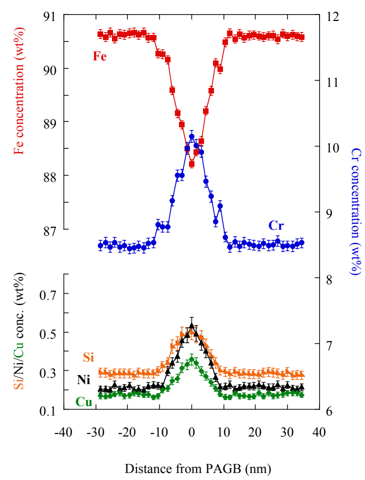

T91_7dpa_400C_01-12_M_2-1-F

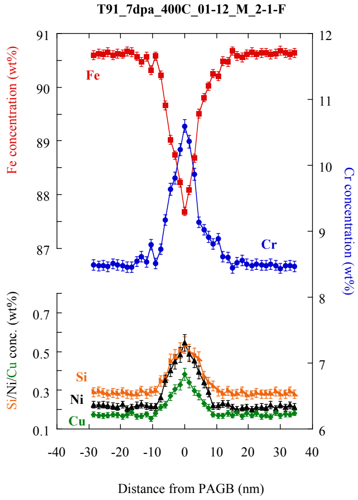

T91_7dpa_400C_01-12_M_2-2-F

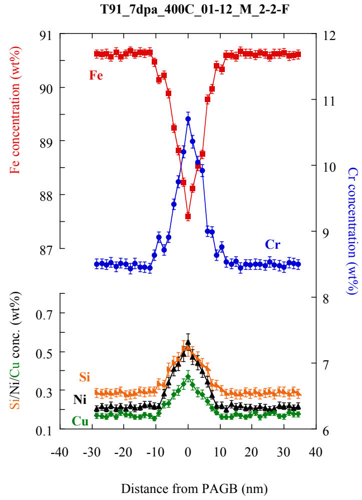

T91_7dpa_400C_01-12_M_2-3-F

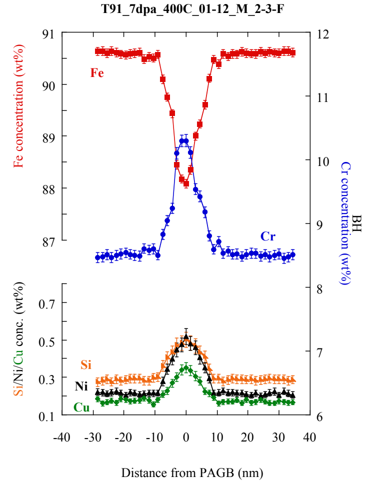

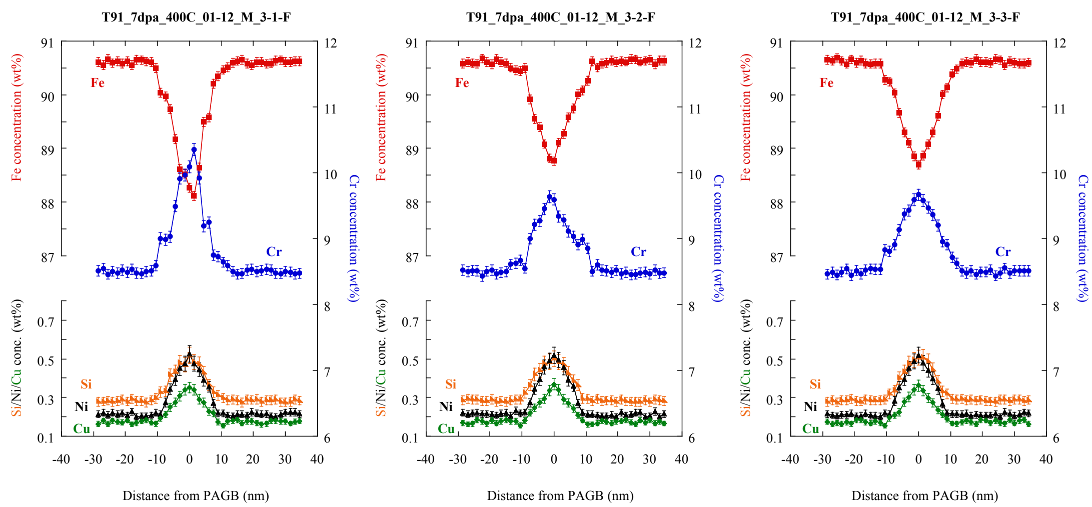
T91_7dpa_400C_01-12_M_3-1-F
T91_7dpa_400C_01-12_M_3-2-F
T91_7dpa_400C_01-12_M_3-3-F
Fe concentration (wt%)
Cr concentration (wt%)
Si/Ni/Cu conc. (wt%)
Fe
Cr
Si
Ni
Cu
Distance from PAGB (nm)

T91_10dpa_400C_01-08

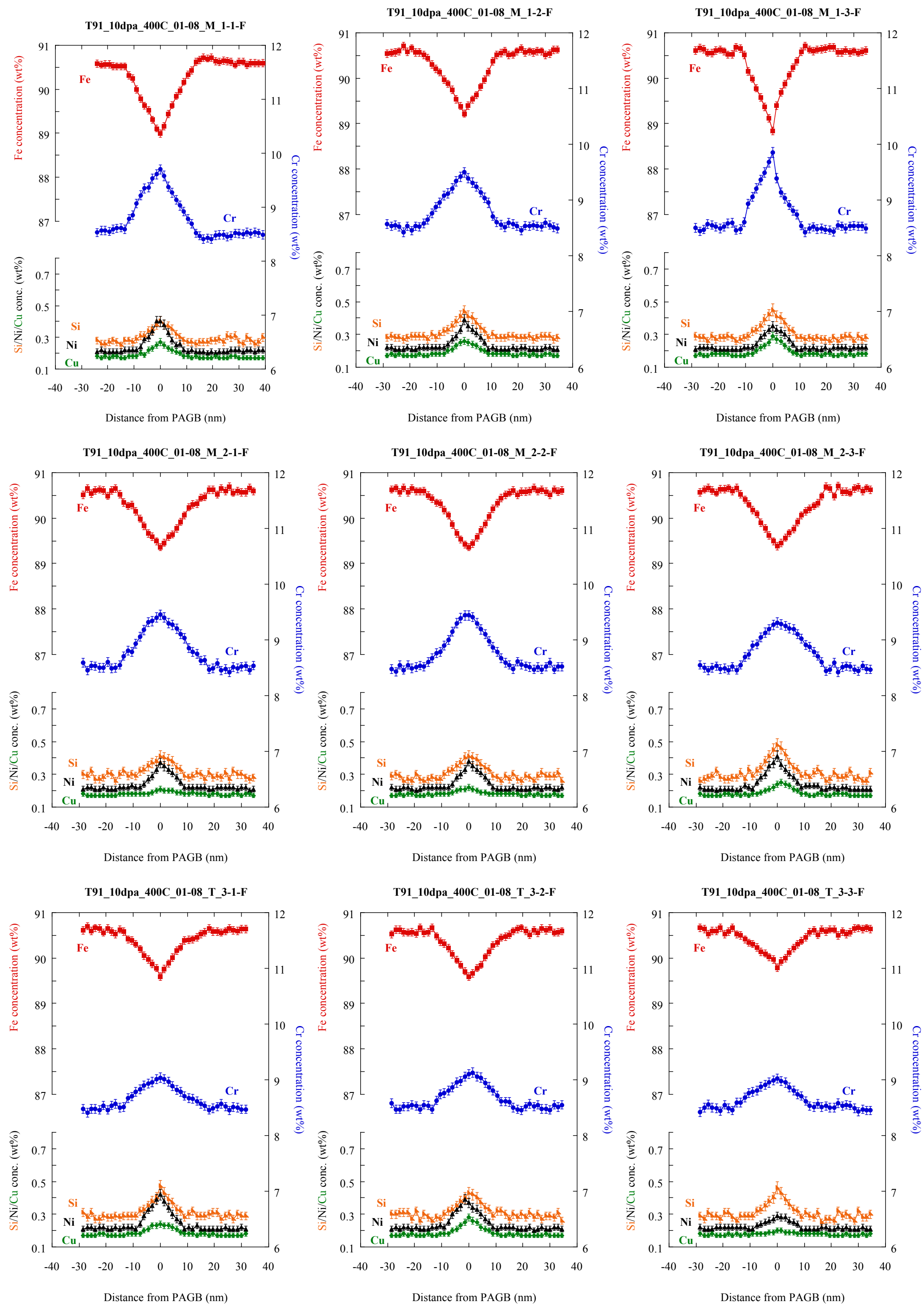

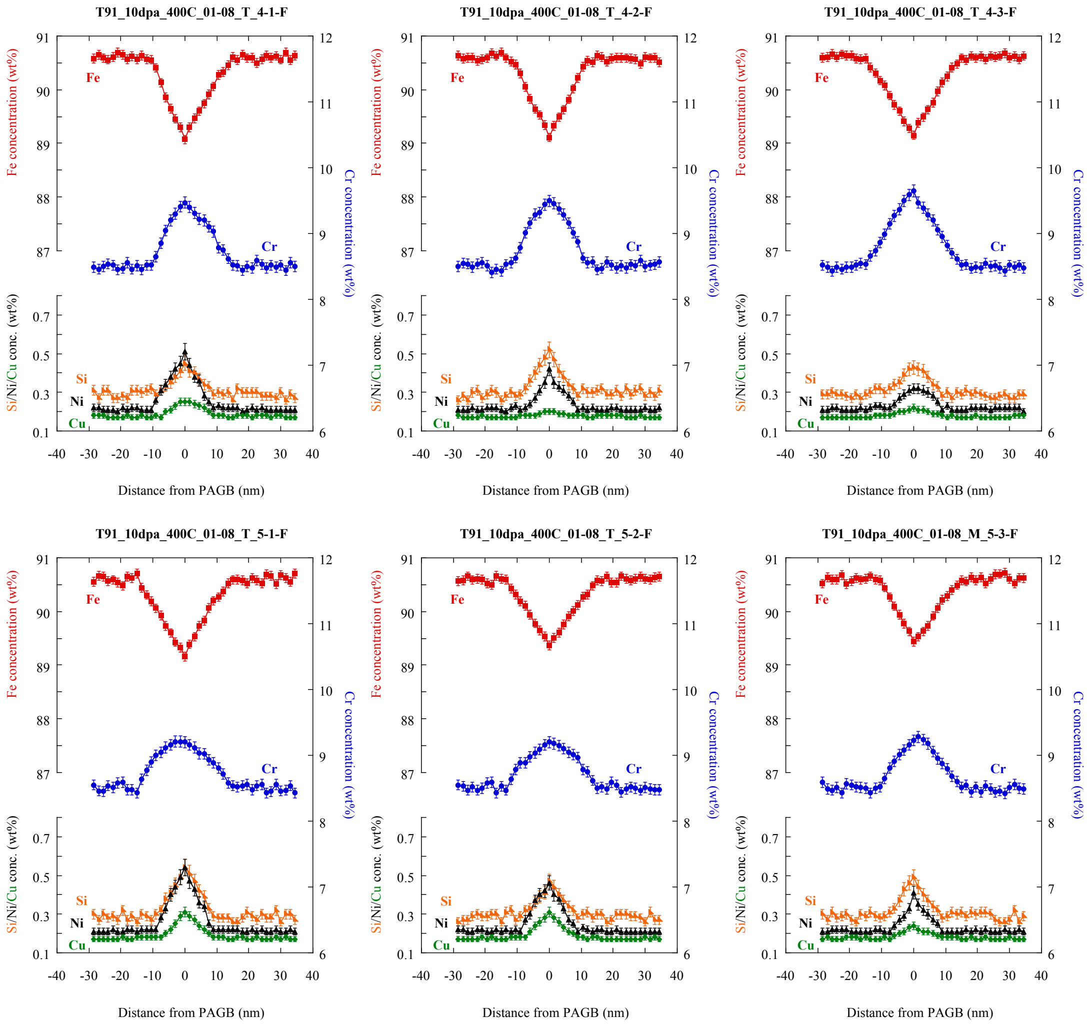
T91_10dpa_400C_01-08_T_4-1-F
T91_10dpa_400C_01-08_T_4-2-F
T91_10dpa_400C_01-08_T_4-3-F
T91_10dpa_400C_01-08_T_5-1-F
T91_10dpa_400C_01-08_T_5-2-F
T91_10dpa_400C_01-08_M_5-3-F
Fe
Cr
Si
Ni
Cu
Fe concentration (wt%)
Cr concentration (wt%)
Si/Ni/Cu conc. (wt%)
Distance from PAGB (nm)

T91_3dpa_450C_10-11

T91_3dpa_450C_10-11_M_1-1-F

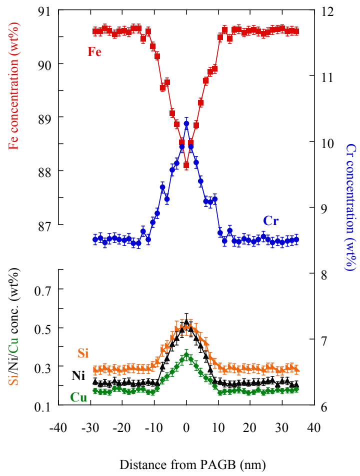

T91_3dpa_450C_10-11_M_1-2-F

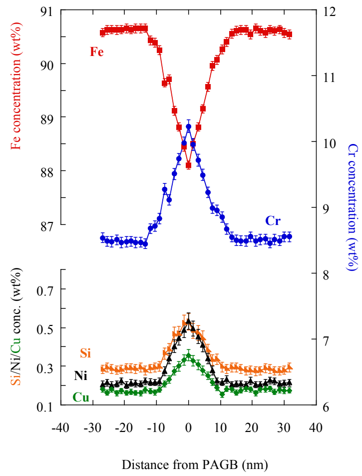

T91_3dpa_450C_10-11_M_1-3-F

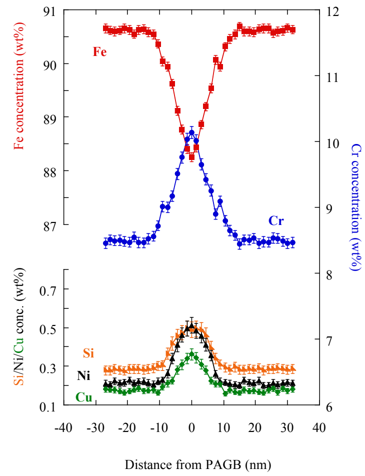

T91_3dpa_450C_10-11_M_1-4-F

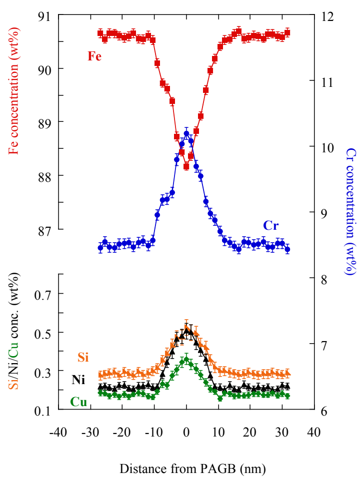

T91_3dpa_450C_10-11_M_1-5-S

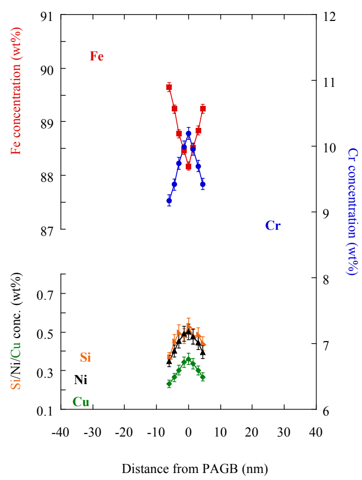

T91_3dpa_450C_10-11_M_1-6-S

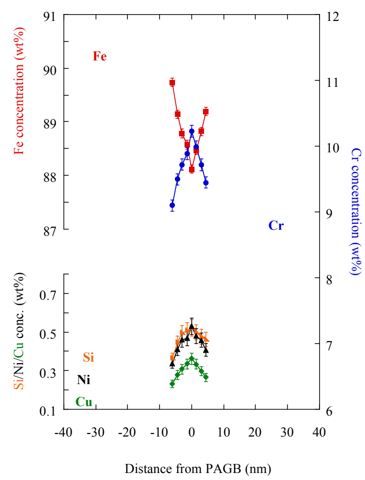

T91_3dpa_450C_10-11_M_1-7-S

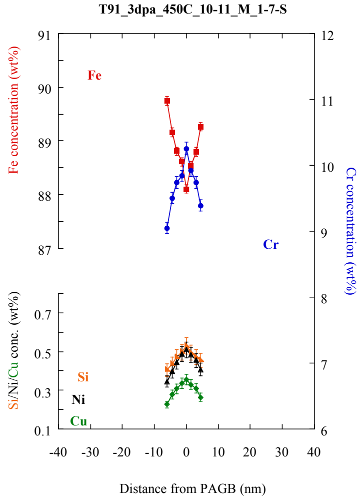

T91_3dpa_450C_10-11_M_1-8-S

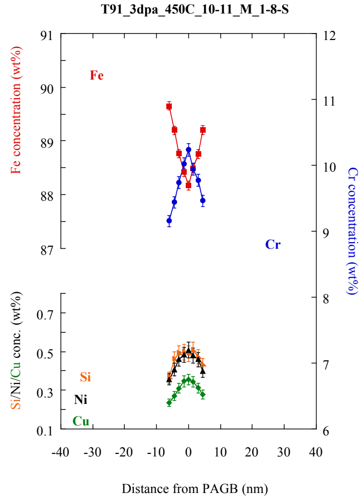

T91_3dpa_450C_10-11_M_1-9-S

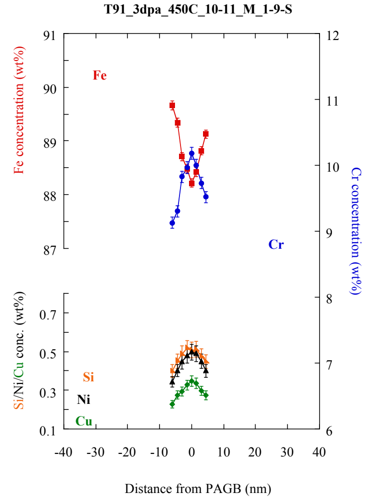

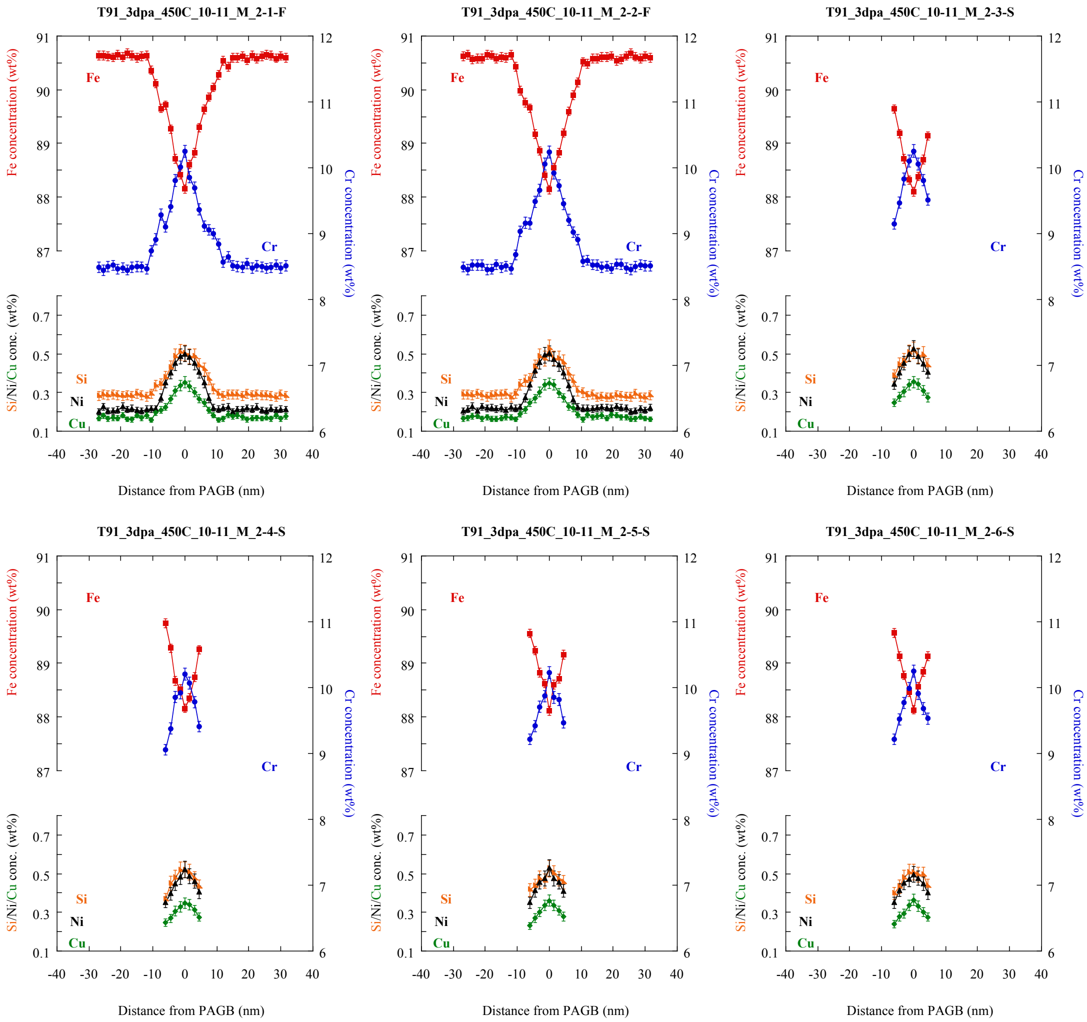
T91_3dpa_450C_10-11_M_2-1-F
T91_3dpa_450C_10-11_M_2-2-F
T91_3dpa_450C_10-11_M_2-3-S
T91_3dpa_450C_10-11_M_2-4-S
T91_3dpa_450C_10-11_M_2-5-S
T91_3dpa_450C_10-11_M_2-6-S
Fe concentration (wt%)
Cr concentration (wt%)
Si/Ni/Cu conc. (wt%)
Fe
Cr
Si
Ni
Cu
Distance from PAGB (nm)

T91_3dpa_500C_07-08

T91_3dpa_500C_07-08_B_1-1-F

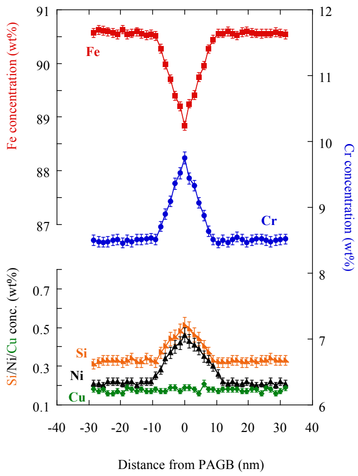

T91_3dpa_500C_07-08_B_1-2-F

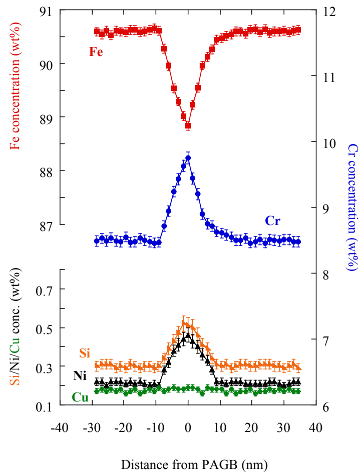

T91_3dpa_500C_07-08_T_2-1-F

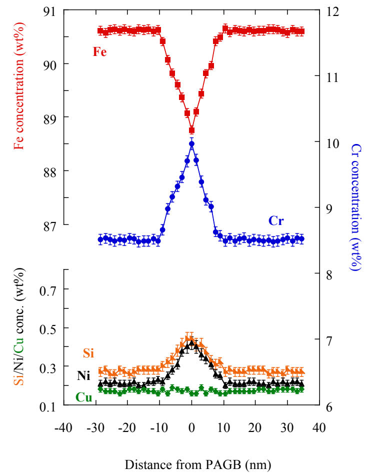

T91_3dpa_500C_07-08_T_2-2-F

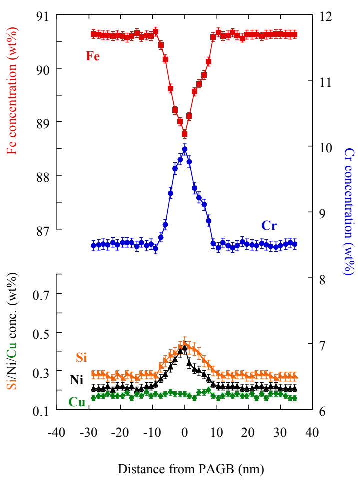

T91_3dpa_500C_07-08_T_2-3-F

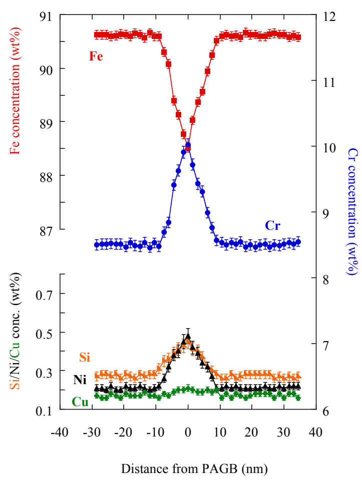

T91_3dpa_500C_07-08_T_2-4-F

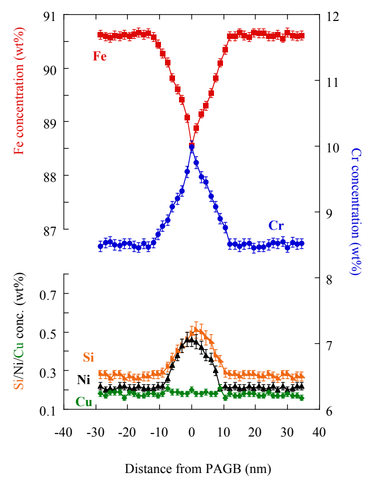

T91_3dpa_600C_01-12

T91_3dpa_600C_01-12_B_1-1-F

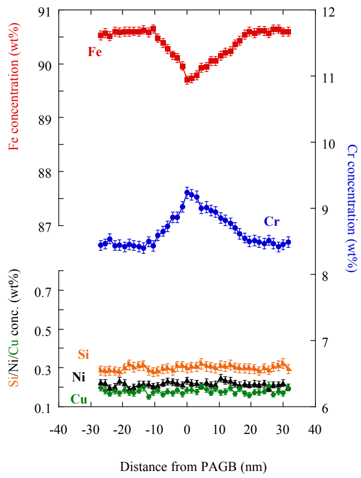

T91_3dpa_600C_01-12_B_1-2-F

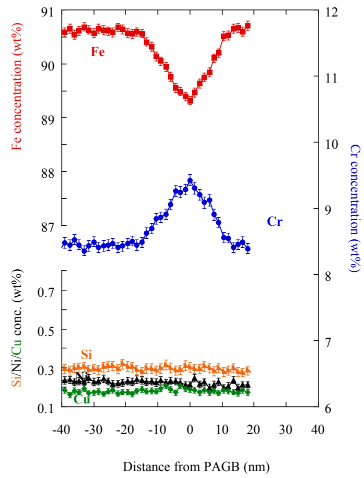

T91_3dpa_600C_01-12_B_1-3-F

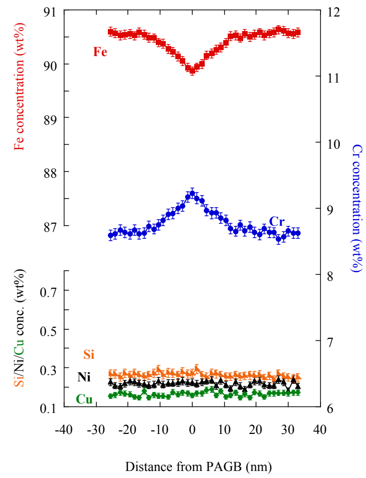

T91_3dpa_600C_01-12_B_2-1-F

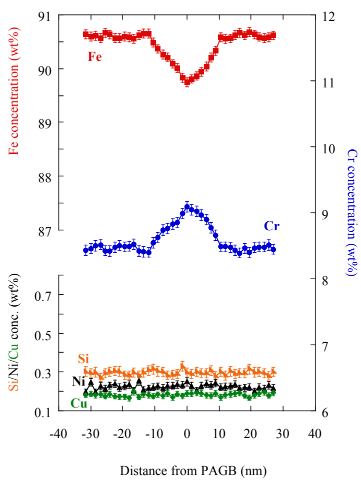

T91_3dpa_600C_01-12_B_2-2-F

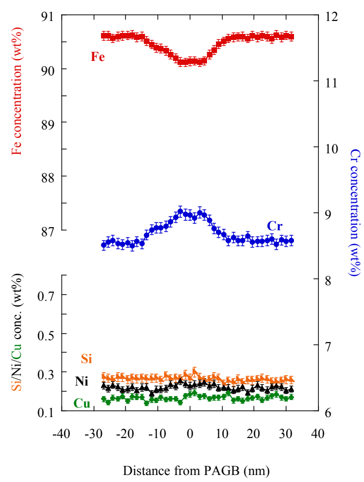

T91_3dpa_600C_01-12_B_2-3-S

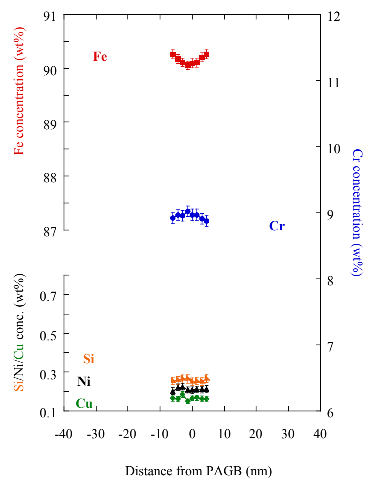

T91_3dpa_600C_01-12_B_2-4-S

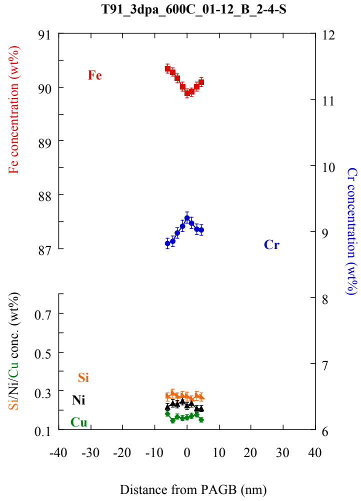

T91_3dpa_700C_05-12

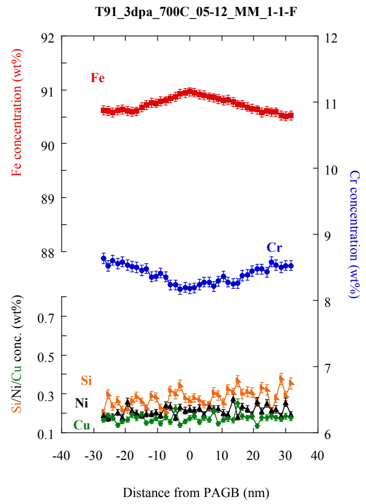

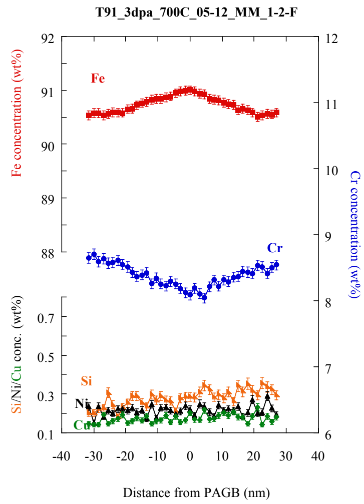

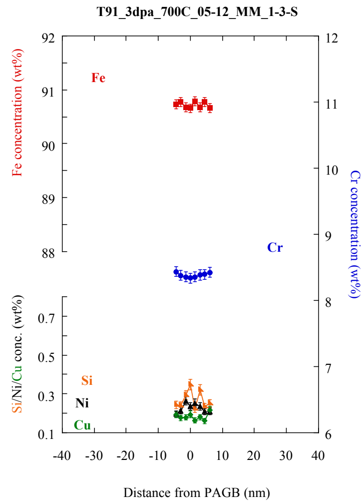

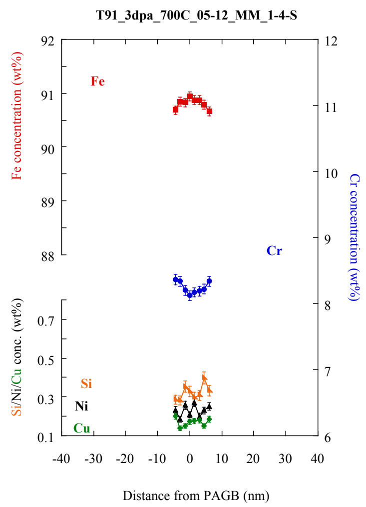

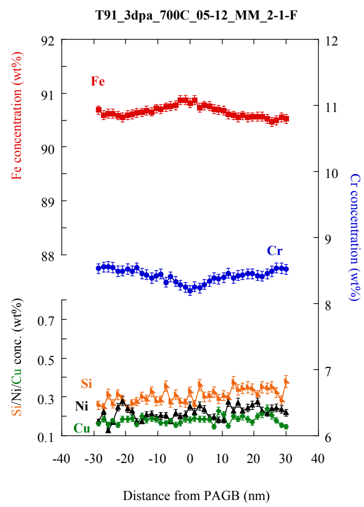

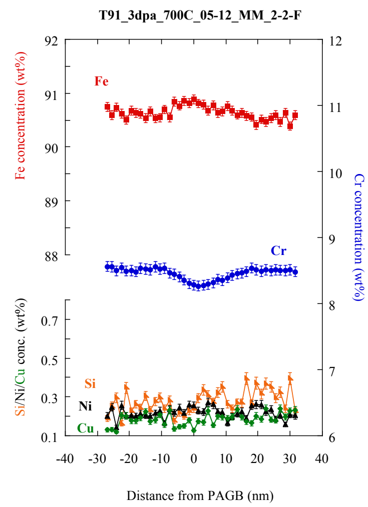

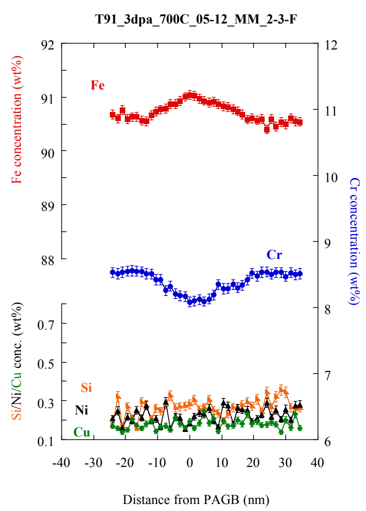

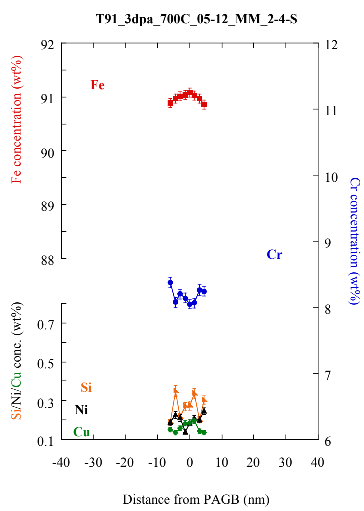

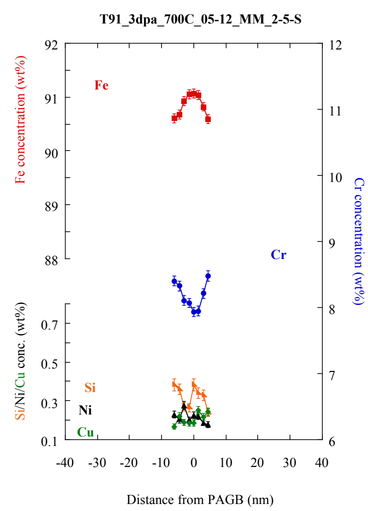

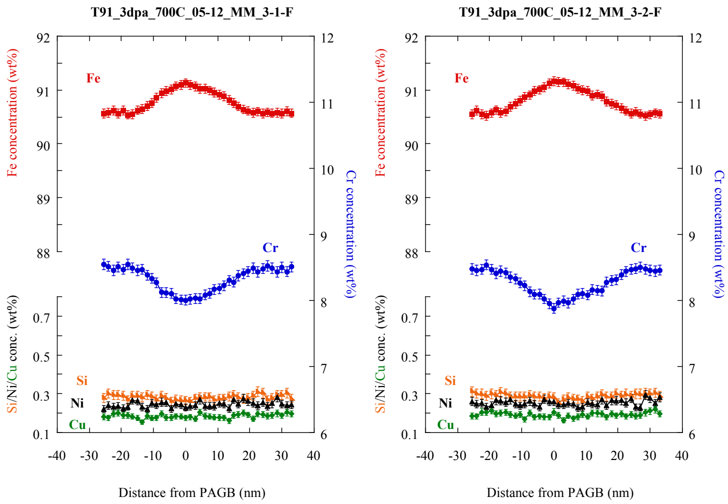
T91_3dpa_700C_05-12_MM_3-1-F
T91_3dpa_700C_05-12_MM_3-2-F
Fe
Cr
Si
Ni
Cu
Fe concentration (wt%)
Cr concentration (wt%)
Si/Ni/Cu conc. (wt%)
Distance from PAGB (nm)

9Cr_1dpa_400C_04-09

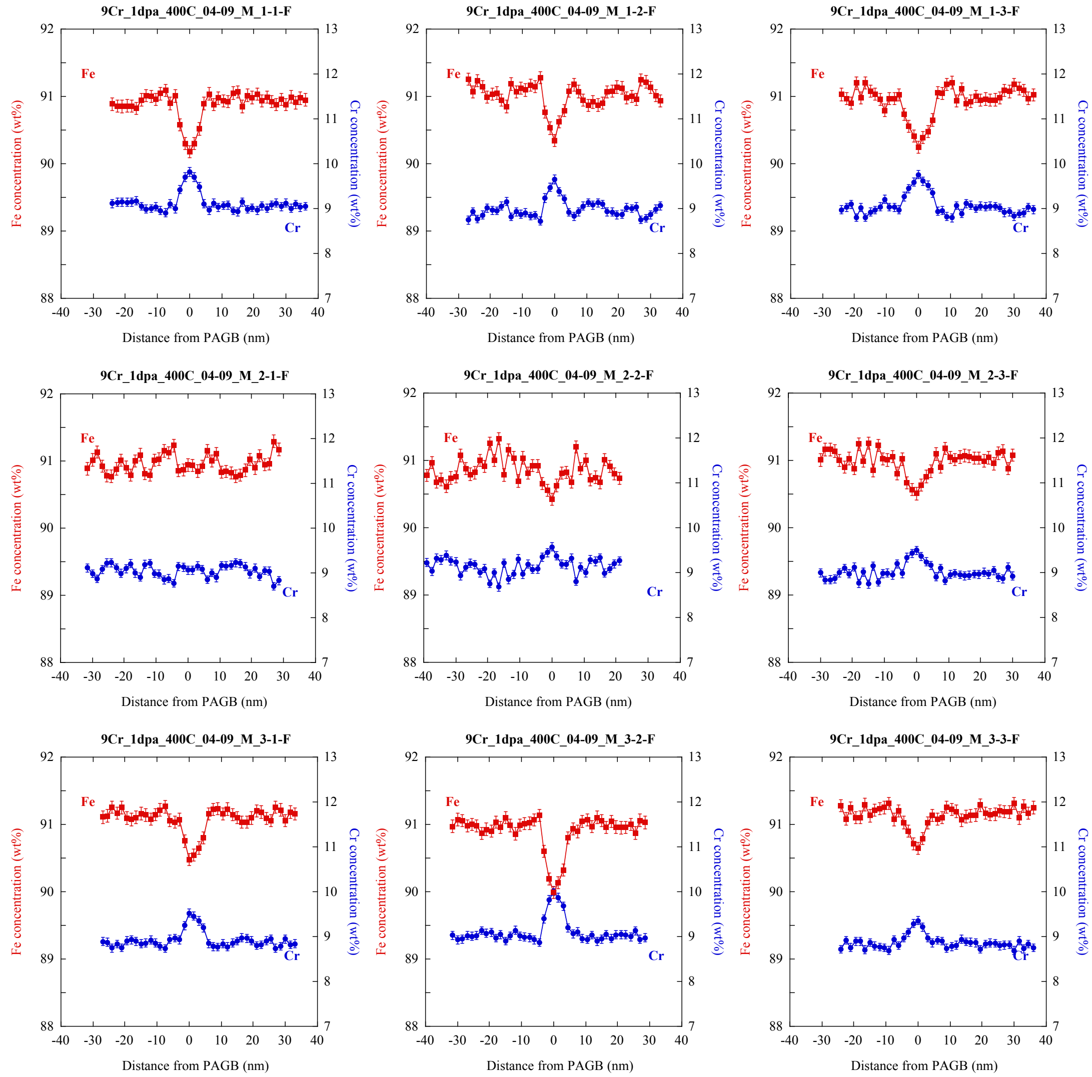

9Cr_3dpa_400C_01-12

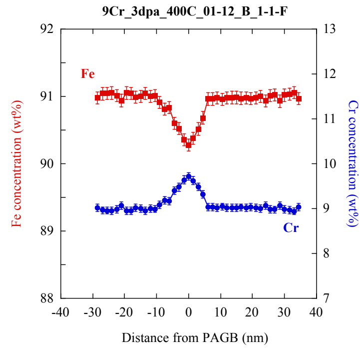

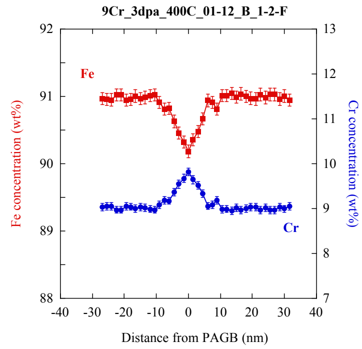

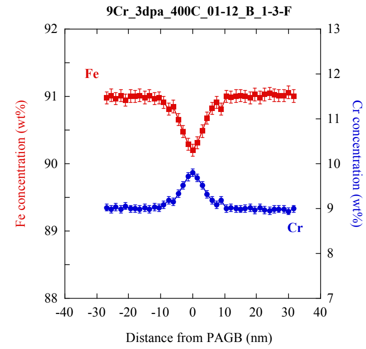

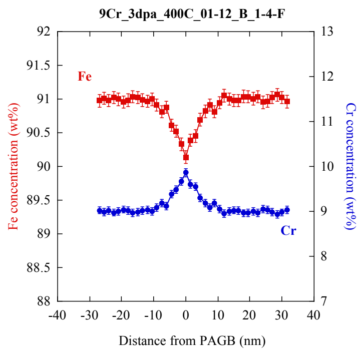

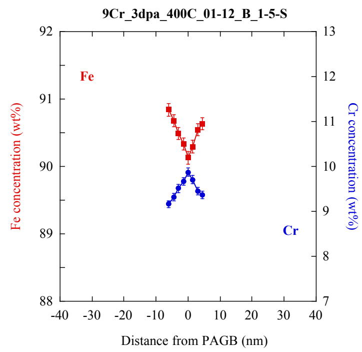

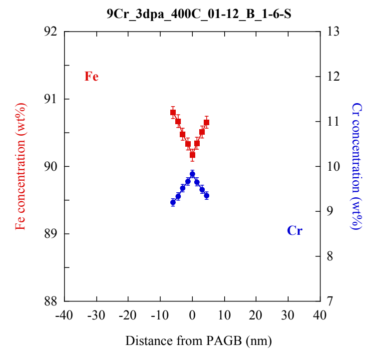

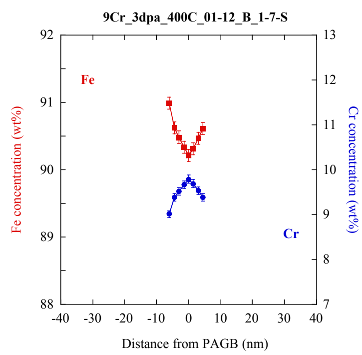

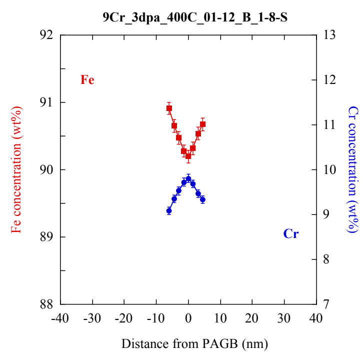

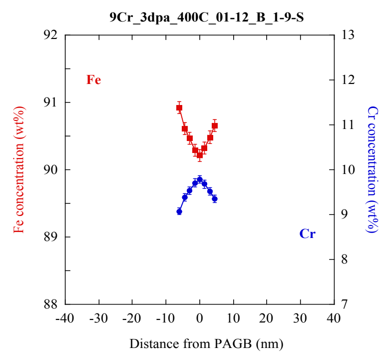

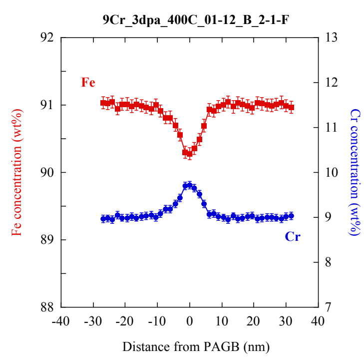

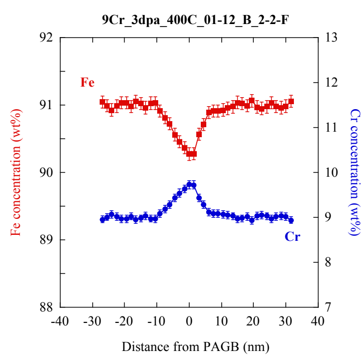

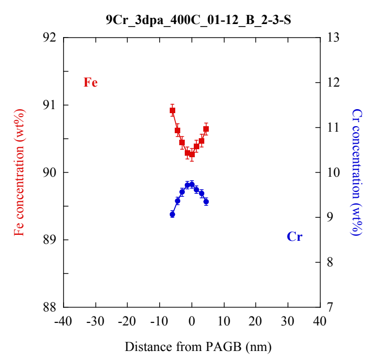

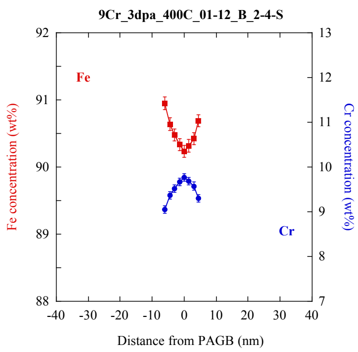
9Cr_3dpa_400C_01-12_B_2-4-S
Fe
Cr
Fe concentration (wt%)
Cr concentration (wt%)
Distance from PAGB (nm)

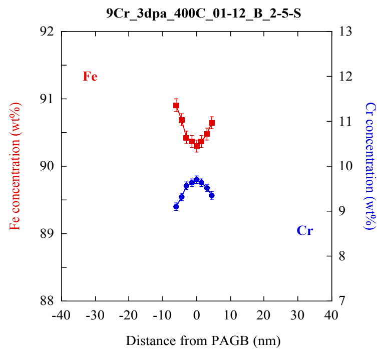
9Cr_3dpa_400C_01-12_B_2-5-S
Fe
Cr
Fe concentration (wt%)
Cr concentration (wt%)
Distance from PAGB (nm)

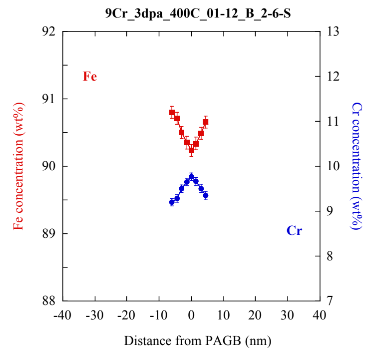
9Cr_3dpa_400C_01-12_B_2-6-S
Fe
Cr
Fe concentration (wt%)
Cr concentration (wt%)
Distance from PAGB (nm)

9Cr_7dpa_400C_04-09

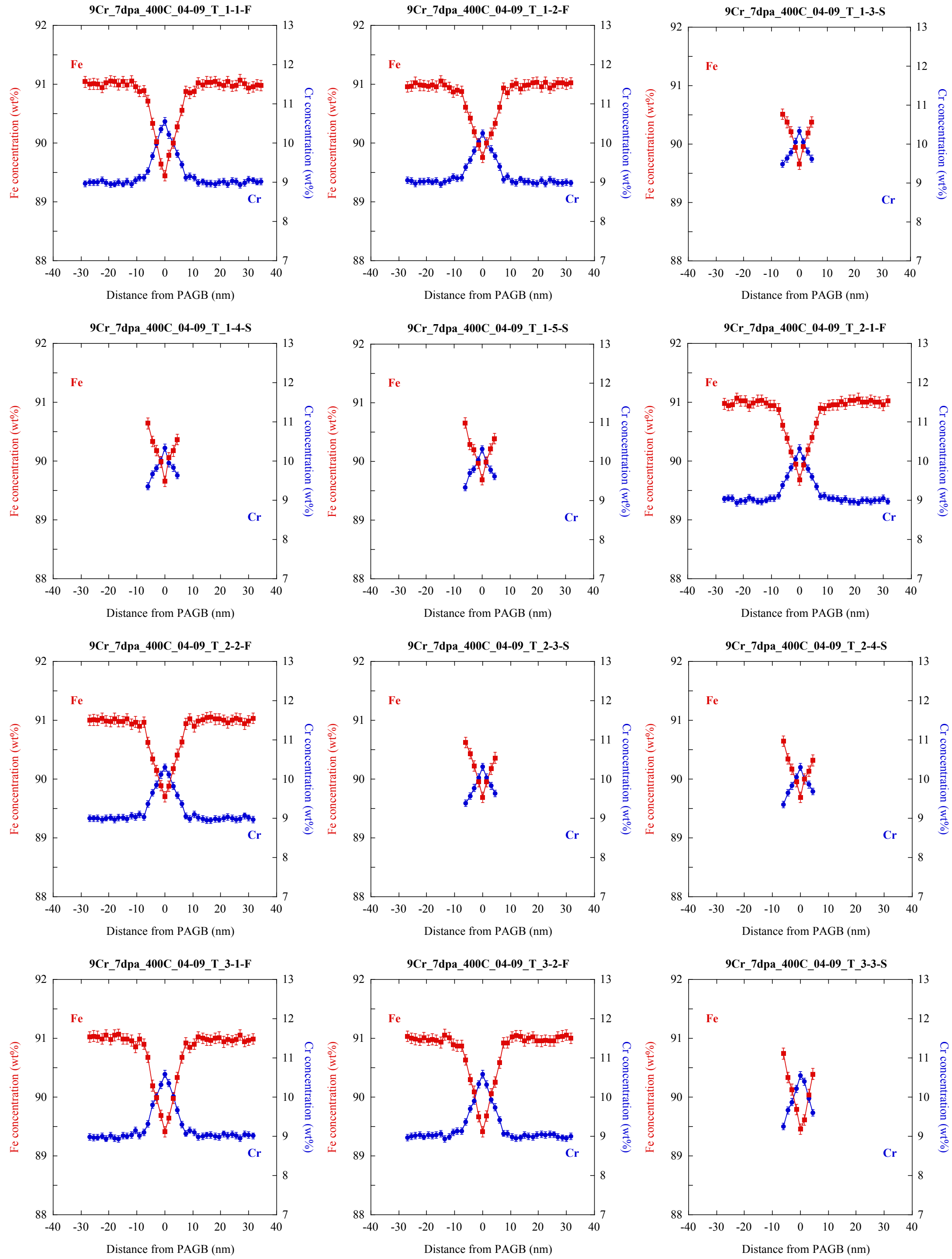

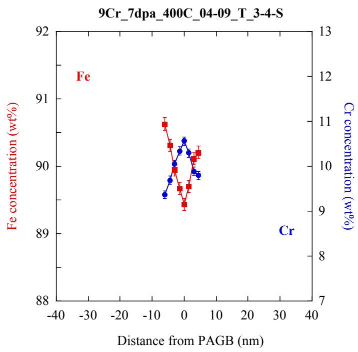
9Cr_7dpa_400C_04-09_T_3-4-S
Fe
Cr
Fe concentration (wt%)
Cr concentration (wt%)
Distance from PAGB (nm)

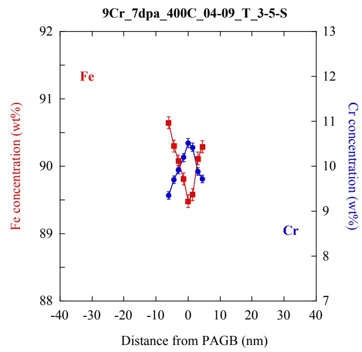
9Cr_7dpa_400C_04-09_T_3-5-S
Fe
Cr
Fe concentration (wt%)
Cr concentration (wt%)
Distance from PAGB (nm)

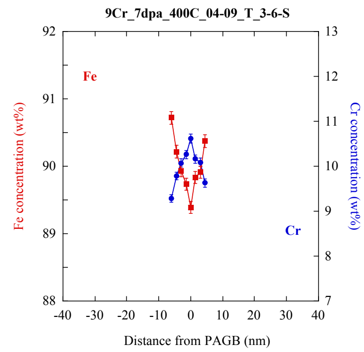
9Cr_7dpa_400C_04-09_T_3-6-S
Fe
Cr
Fe concentration (wt%)
Cr concentration (wt%)
Distance from PAGB (nm)

9Cr_10dpa_400C_01-12

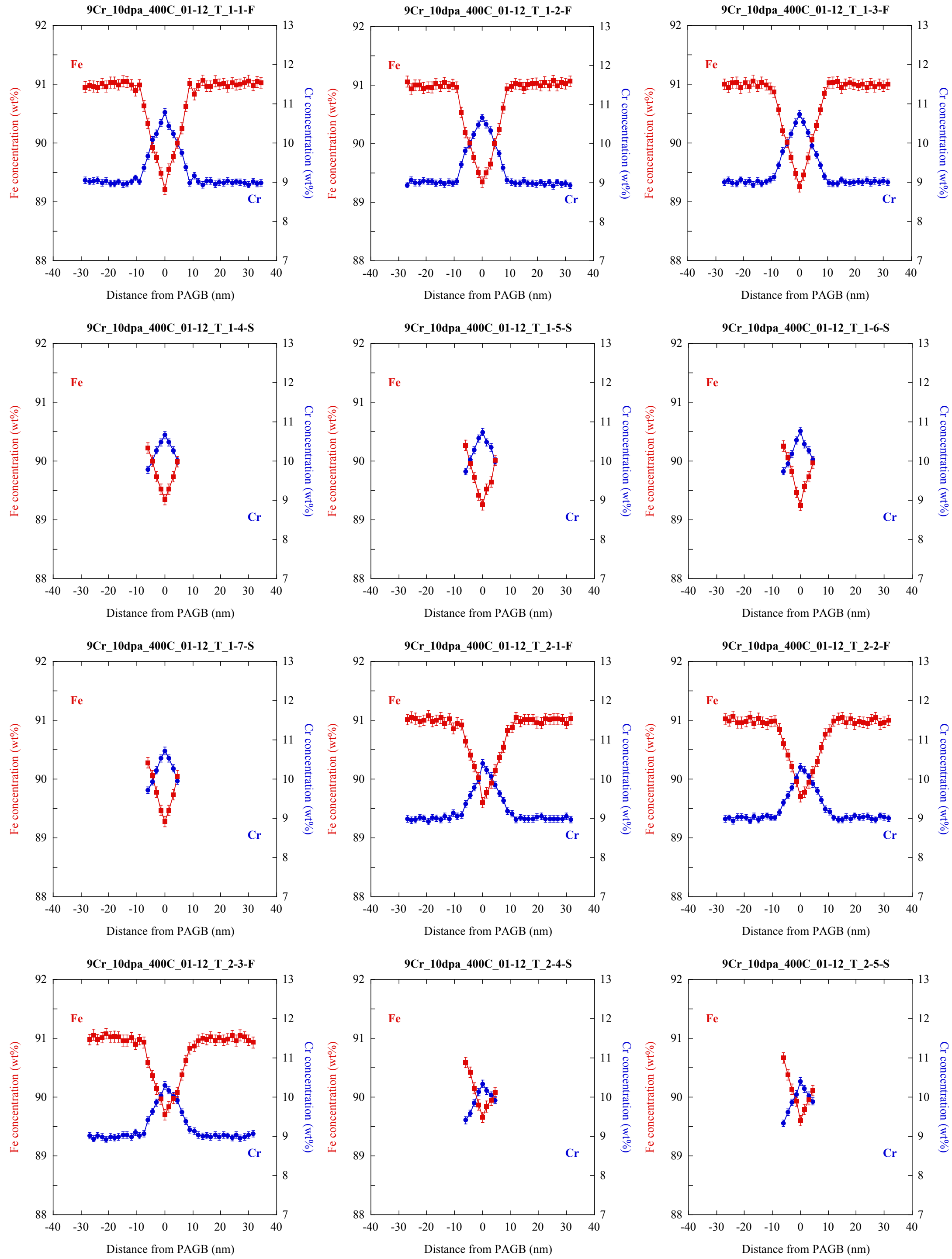

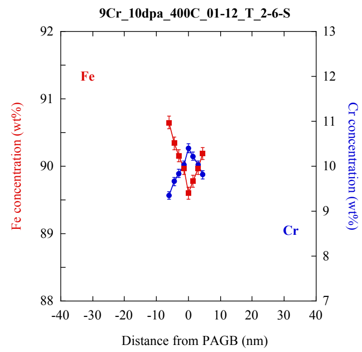
9Cr_10dpa_400C_01-12_T_2-6-S
Fe
Cr
Fe concentration (wt%)
Cr concentration (wt%)
Distance from PAGB (nm)
92
91
90
89
88
13
12
11
10
9
8
7
-40
-30
-20
-10
0
10
20
30
40

HT9_3dpa_400C_12-07

HT9_3dpa_400C_12-07_M_1-1-F

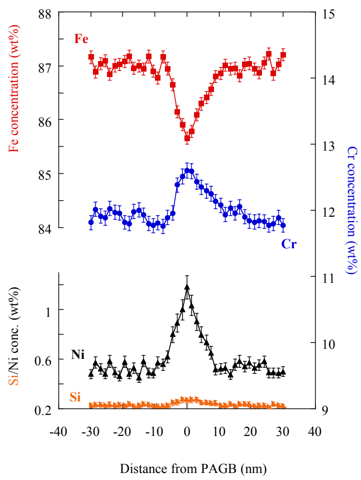

HT9_3dpa_400C_12-07_M_1-2-F

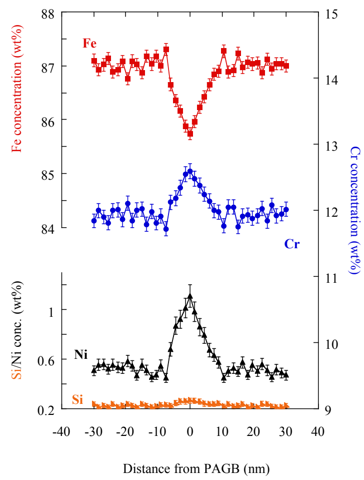

HT9_3dpa_400C_12-07_M_2-1-F

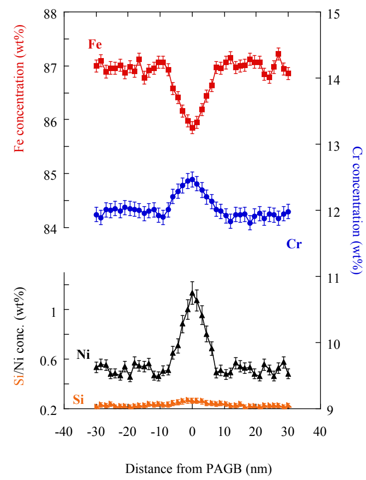

HT9_3dpa_400C_12-07_M_2-2-F

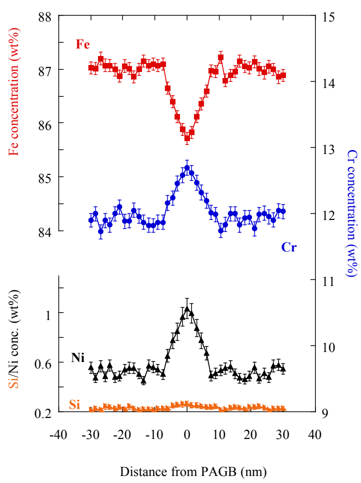

HT9_3dpa_400C_12-07_B_3-1-F

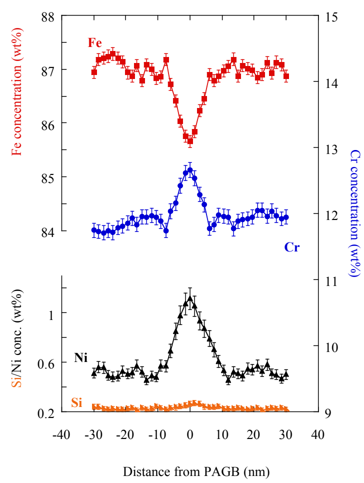

HT9_3dpa_400C_12-07_B_3-2-F

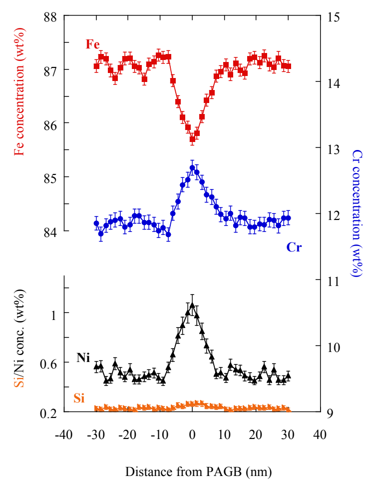

HT9_3dpa_400C_12-07_B_4-1-F

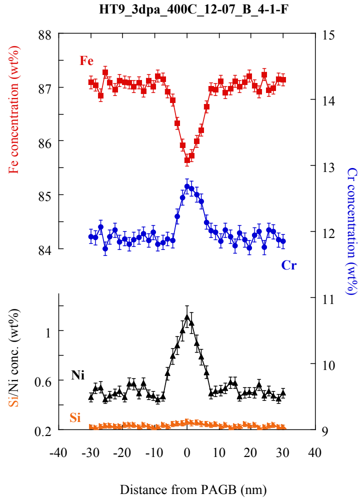

HT9_3dpa_400C_12-07_B_4-2-F

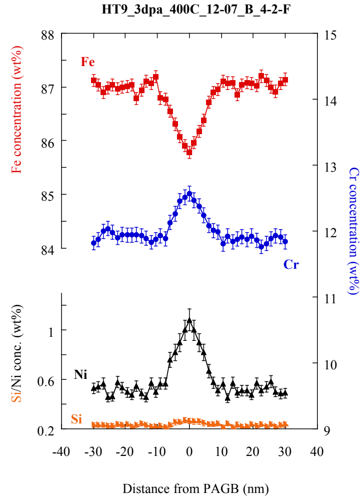

HCM12A_3dpa_400C_12-07

HCM12A_3dpa_400C_12-07_M_1-1-F

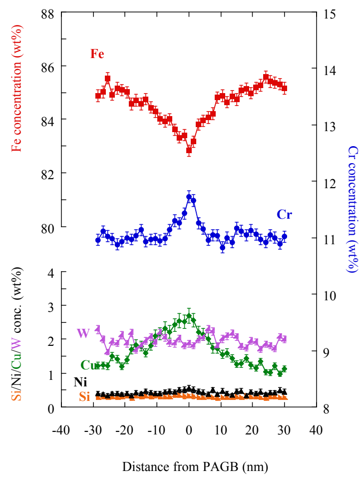

HCM12A_3dpa_400C_12-07_M_1-2-F

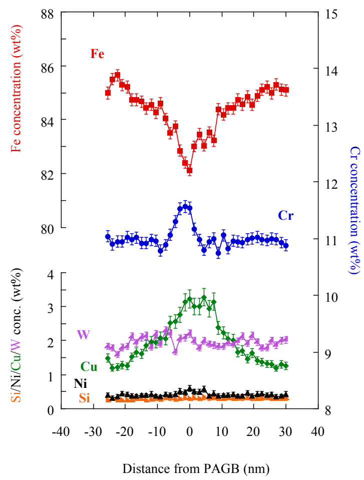

HCM12A_3dpa_400C_12-07_M_1-3-F

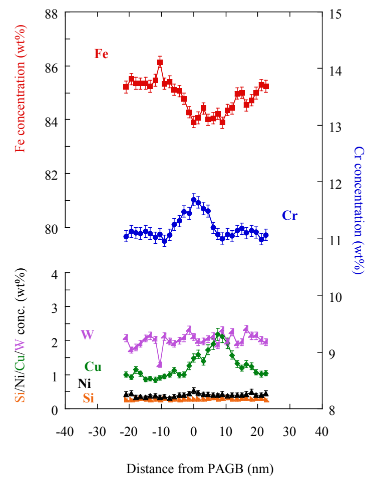

HCM12A_3dpa_400C_12-07_M_2-1-F

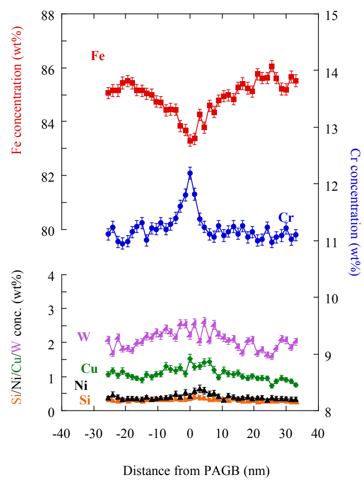

HCM12A_3dpa_400C_12-07_M_2-2-F

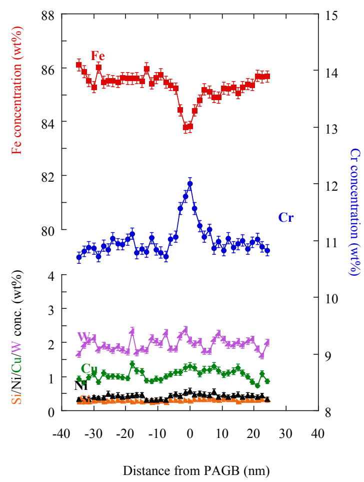

HCM12A_3dpa_400C_12-07_M_2-3-F

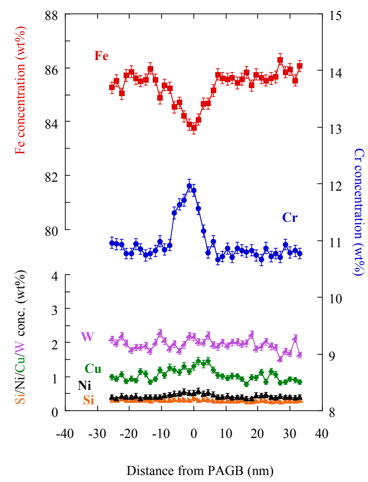

HCM12A_3dpa_400C_12-07_M_2-4-F

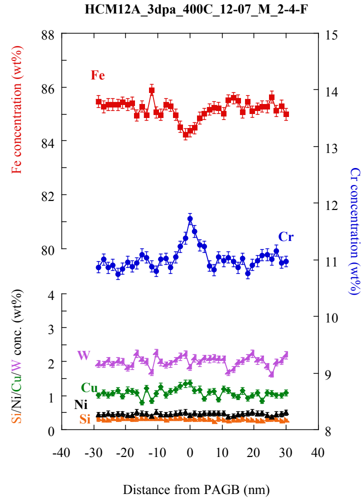

BIBLIOGRAPHY

[1] R. L. Klueh and D. R. Harries, *High-Chromium Ferritic and Martensitic Steels for Nuclear Applications*. ASTM, 2001.

[2] A. Kostka, K. Tak, R. Hellmig, Y. Estrin, and G. Eggeler, "On the contribution of carbides and micrograin boundaries to the creep strength of tempered martensite ferritic steels," *Acta Materialia*, vol. 55, no. 2, pp. 539–550, Jan. 2007.

[3] H. Takahashi, S. Ohnuki, and T. Takeyama, "Radiation-induced segregation at internal sinks in electron irradiated binary alloys," *Journal of Nuclear Materials*, vol. 103–104, pp. 1415–1420, 1981.

[4] T. Kato, H. Takahashi, S. Ohnuki, K. Nakata, and J. Kuniya, "The effect of solute content on grain boundary in electron-irradiated Fe-Cr-Mn alloys," *Journal of Nuclear Materials*, vol. 179–181, pp. 623–625, 1991.

[5] S. Ohnuki, H. Takahashi, and T. Takeyama, "Void swelling and segregation of solute in ion-irradiated ferritic steels," *Journal of Nuclear Materials*, vol. 103–104, pp. 1121–1125, 1981.

[6] R. E. Clausing, L. Heatherly, R. G. Faulkner, A. F. Rowcliffe, and K. Farrell, "Radiation-induced segregation in HT-9 martensitic steel," *Journal of Nuclear Materials*, vol. 141–143, pp. 978–981, 1986.

[7] E. A. Little, T. S. Morgan, and R. G. Faulkner, "Microchemistry of neutron irradiated 12%CrMoVNb martensitic steel," *Materials Science Forum*, vol. 97–99, pp. 323–328, 1992.

[8] Y. Hamaguchi, H. Kuwano, H. Kamide, R. Miura, and T. Yamada, "Effects of proton irradiation on the hardening behavior of HT-9 steel," *Journal of Nuclear Materials*, vol. 133–134, pp. 636–639, 1985.

[9] I. Neklyudov and V. Voyevodin, "Features of structure-phase transformations and segregation processes under irradiation of austenitic and ferritic-martensitic steels," *Journal of Nuclear Materials*, vol. 212–215, pp. 39–44, Sep. 1994.

[10] R. Schaeublin, P. Spatig, and M. Victoria, "Chemical segregation behavior of the low activation ferritic / martensitic steel F82H," *Journal of Nuclear Materials*, vol. 263, pp. 1350–1355, 1998.

[11] G. Gupta, Z. Jiao, A. N. Ham, J. T. Busby, and G. S. Was, "Microstructural evolution of proton irradiated T91," *Journal of Nuclear Materials*, vol. 351, no. 1–3, pp. 162–173, Jun. 2006.

[12] Z. Lu, R. Faulkner, N. Sakaguchi, H. Kinoshita, H. Takahashi, and P. Flewitt, "Effect of hafnium on radiation-induced inter-granular segregation in ferritic steel," *Journal of Nuclear Materials*, vol. 351, no. 1–3, pp. 155–161, Jun. 2006.

[13] E. a. Marquis, S. Lozano-Perez, and V. D. Castro, “Effects of heavy-ion irradiation on the grain boundary chemistry of an oxide-dispersion strengthened Fe–12wt.% Cr alloy,” *Journal of Nuclear Materials*, vol. 417, pp. 257–261, Oct. 2011.
[14] E. a. Marquis, R. Hu, and T. Rousseau, “A systematic approach for the study of radiation-induced segregation/depletion at grain boundaries in steels,” *Journal of Nuclear Materials*, vol. 413, no. 1, pp. 1–4, Jun. 2011.
[15] T. R. Allen, J. T. Busby, G. S. Was, and E. A. Kenik, “On the mechanism of radiation-induced segregation in austenitic Fe–Cr–Ni alloys,” *Journal of Nuclear Materials*, vol. 255, pp. 44–58, 1998.
[16] J. T. Busby, G. S. Was, and E. A. Kenik, “Isolating the effect of radiation-induced segregation in irradiation-assisted stress corrosion cracking of austenitic stainless steels,” *Journal of Nuclear Materials*, vol. 302, pp. 20–40, Apr. 2002.
[17] J. M. Perks and S. M. Murphy, “Modelling the major element radiation-induced segregation in concentrated Fe-Cr-Ni alloys,” in *Materials for Nuclear Reactor Core Applications, Vol. 1, Bristol, UK*, pp. 165–169.
[18] T. R. Allen and G. S. Was, “Modeling radiation-induced segregation in austenitic Fe–Cr–Ni alloys,” *Acta Materialia*, vol. 46, no. 10, pp. 3679–3691, Jun. 1998.
[19] G. S. Was, *Fundamentals of Radiation Materials Science: Metals and Alloys*. Springer, 2007.
[20] G. S. Was and S. M. Bruemmer, “Effects of irradiation on intergranular stress corrosion cracking,” *Journal of Nuclear Materials*, vol. 216, pp. 326–347, Oct. 1994.
[21] G. S. Was and T. R. Allen, “Radiation-Induced Segregation in Multicomponent Alloys: Effect of Particle Type,” *Materials Characterization*, vol. 32, pp. 239–255, Jun. 1994.
[22] J. H. Westbrook and K. T. Aust, “Solute hardening at interfaces in high-purity lead - I. Grain and twin boundaries,” *Acta Metallurgica*, vol. 11, p. 1151, 1963.
[23] K. T. Aust and J. H. Westbrook, *Lattice Defects in Quenched Metals*. Academic Press, 1965, p. 771.
[24] K. T. Aust, A. J. Peat, and J. H. Westbrook, “Quench-hardening gradients near vacancy sinks in crystals of zone refined lead,” *Acta Metallurgica*, vol. 14, p. 1469, 1966.
[25] K. T. Aust, R. E. Hanneman, P. Niessen, and J. H. Westbrook, “Solute induced hardening near grain boundaries in zone refined metals,” *Acta Metallurgica*, vol. 16, p. 291, 1968.
[26] R. E. Howard and A. B. Lidiard, “The annealing of vacancies in dilute alloys,” *Philosophical Magazine*, vol. 11, pp. 1179–1188, 1965.
[27] T. R. Anthony and R. E. Hanneman, “Non-Equilibrium Segregation of Impurities in Quenched Dilute Alloys,” *Scripta Metallurgica*, vol. 2, pp. 611–614, 1968.
[28] T. R. Anthony, “Solute segregation in vacancy gradients generated by sintering and temperature changes,” *Acta Materialia*, vol. 17, p. 603, 1969.
[29] T. R. Anthony, “Solute segregation and stresses generated around growing voids in metals,” in *Radiation-induced voids in metals*, 1972, vol. 15, pp. 630–646.
[30] P. R. Okamoto and H. Wiedersich, “Segregation of alloying elements to free surfaces during irradiation,” *Journal of Nuclear Materials*, vol. 53, pp. 336–345, 1974.

[31] R. A. Johnson and N. Q. Lam, “Solute segregation in metals under irradiation,” *Physical Review B*, vol. 13, no. 10, pp. 4364–4375, 1976.
[32] P. R. Okamoto and L. E. Rehn, “Radiation-induced segregation in binary and ternary alloys,” *Journal of Nuclear Materials*, vol. 83, pp. 2–23, 1979.
[33] P. G. Shewmon, “Surface Diffusion from a Point Source,” *Journal of Applied Physics*, vol. 34, no. 4, p. 755, 1963.
[34] A. D. Marwick, “Segregation in irradiated alloys: the inverse Kirkendall effect and the effect of constitution on void swelling,” *J. Phys. F: Metal Phys.*, vol. 8, no. 9, pp. 1849–1961, 1978.
[35] H. Wiedersich, P. R. Okamoto, and N. Q. Lam, “A theory of radiation-induced segregation in concentrated alloys,” *Journal of Nuclear Materials*, vol. 83, pp. 98–108, 1979.
[36] N. Q. Lam, A. Kumar, and H. Wiedersich, “Kinetics of radiation-induced segregation in ternary alloys,” in *Effects of Radiation on Materials: Eleventh Conference*, 1982, vol. 15, pp. 985–1007.
[37] J. M. Perks, A. D. Marwick, and C. A. English, “A Computer Code to Calculate Radiation-Induced Segregation in Concentrated Ternary Alloys,” *Materials Development Division, Harwell Laboratory, AERE-R 12121*.
[38] S. Watanabe, N. Sakaguchi, N. Hashimoto, and H. Takahashi, “Quantitative studies of irradiation-induced segregation and grain boundary migration in FeCrNi alloy,” *Journal of Nuclear Materials*, vol. 224, no. 2, pp. 158–168, Aug. 1995.
[39] S. Watanabe and H. Takahashi, “Discriminant of RIS in multi-component alloys,” *Journal of Nuclear Materials*, vol. 208, no. 1–2, pp. 191–194, Jan. 1994.
[40] M. J. Hackett, “Mechanism for Suppression of Radiation-Induced Segregation by Oversized Solute Addition in Austenitic Stainless Steel,” University of Michigan, 2008.
[41] M. J. Hackett, R. Najafabadi, and G. S. Was, “Modeling solute-vacancy trapping at oversized solutes and its effect on radiation-induced segregation in Fe–Cr–Ni alloys,” *Journal of Nuclear Materials*, vol. 389, no. 2, pp. 279–287, May 2009.
[42] J. R. Manning, “Correlation factors for diffusion in nondilute alloys,” *Physical Review B*, vol. 4, no. 4, pp. 1111–1121, 1971.
[43] L. E. Rehn, P. R. Okamoto, D. I. Potter, and H. Wiedersich, “Effect of solute misfit and temperature on irradiation-induced segregation in binary Ni alloys,” *Journal of Nuclear Materials*, vol. 74, pp. 242–251, 1978.
[44] R. Faulkner, N. Waite, E. Little, and T. Morgan, “Radiation-induced grain boundary segregation in dilute alloys,” *Materials Science and Engineering: A*, vol. 171, no. 1–2, pp. 241–248, Nov. 1993.
[45] R. G. Faulkner, S. Song, and P. E. J. Flewitt, “A Model Describing Neutron Irradiation-Induced Segregation to Grain Boundaries in Dilute Alloys,” *Metallurgical and Materials Transactions A*, vol. 27A, pp. 3381–3390, 1996.
[46] R. Faulkner, “Radiation-induced grain boundary segregation in nuclear reactor steels,” *Journal of Nuclear Materials*, vol. 251, pp. 269–275, Nov. 1997.
[47] R. G. Faulkner, S. Song, P. E. J. Flewitt, M. Victoria, and P. Marmy, “Grain boundary segregation under neutron irradiation in dilute alloys,” *Journal of Nuclear Materials*, vol. 255, pp. 189–209, 1998.

[48] R. . Faulkner, S. Song, and P. E. . Flewitt, “Radiation-induced inter-granular segregation in first wall fusion reactor materials,” *Journal of Nuclear Materials*, vol. 283–287, pp. 147–151, Dec. 2000.
[49] R. G. Faulkner, R. B. Jones, Z. Lu, and P. E. J. Flewitt *, “Grain boundary impurity segregation and neutron irradiation effects in ferritic alloys,” *Philosophical Magazine*, vol. 85, no. 19, pp. 2065–2099, Jul. 2005.
[50] H. Watanabe, T. Muroga, and N. Yoshida, “The effects of oversized solute addition on microstructural evolution in Fe-Cr-Ni alloys during electron irradiation,” *Journal of Nuclear Materials*, vol. 239, pp. 95–98, Dec. 1996.
[51] N. Sakaguchi, S. Watanabe, and H. Takahashi, “Effect of additional minor element on radiation-induced grain boundary segregation in austenitic stainless steel under electron irradiation,” *Nuclear Instruments and Methods in Physics Research Section B: Beam Interactions with Materials and Atoms*, vol. 153, no. 1–4, pp. 142–146, Jun. 1999.
[52] D. I. R. Norris, C. Baker, C. Taylor, and J. M. Titchmarsh, “Radiation-induced segregation in 20Cr/25Ni/Nb stainless steel,” in *Effects of Radiation on Materials: 15th International Conference*, 1992, pp. 603–620.
[53] K. Wong, J. Shim, and B. Wirth, “Molecular dynamics simulations of point defect interactions in Fe–Cr alloys,” *Journal of Nuclear Materials*, vol. 367–370, pp. 276–281, Aug. 2007.
[54] K. L. Wong, H.-J. Lee, J.-H. Shim, B. Sadigh, and B. D. Wirth, “Multiscale modeling of point defect interactions in Fe–Cr alloys,” *Journal of Nuclear Materials*, vol. 386–388, pp. 227–230, Apr. 2009.
[55] S. Choudhury et al., “Ab-initio based modeling of diffusion in dilute bcc Fe–Ni and Fe–Cr alloys and implications for radiation induced segregation,” *Journal of Nuclear Materials*, vol. 411, no. 1–3, pp. 1–14, Apr. 2011.
[56] J. Pešička, R. Kužel, a. Dronhofer, and G. Eggeler, “The evolution of dislocation density during heat treatment and creep of tempered martensite ferritic steels,” *Acta Materialia*, vol. 51, no. 16, pp. 4847–4862, Sep. 2003.
[57] R. Klueh, N. Hashimoto, M. Sokolov, K. Shiba, and S. Jitsukawa, “Mechanical properties of neutron-irradiated nickel-containing martensitic steels: I. Experimental study,” *Journal of Nuclear Materials*, vol. 357, no. 1–3, pp. 156–168, Oct. 2006.
[58] J. Pešička, A. Dronhofer, and G. Eggeler, “Free dislocations and boundary dislocations in tempered martensite ferritic steels,” *Materials Science and Engineering A*, vol. 387–389, pp. 176–180, Dec. 2004.
[59] G. Eggeler, J. C. Earthman, N. Nilsvang, and B. Ilschner, “Microstructural study of creep rupture in a 12% Chromium ferritic steel,” *Acta Metallurgica*, vol. 37, no. 1, pp. 49–60, Jan. 1989.
[60] R. Klueh, K. Shiba, and M. Sokolov, “Embrittlement of irradiated ferritic/martensitic steels in the absence of irradiation hardening,” *Journal of Nuclear Materials*, vol. 377, no. 3, pp. 427–437, Jul. 2008.
[61] X. Jia and Y. Dai, “Microstructure in martensitic steels T91 and F82H after irradiation in SINQ Target-3,” *Journal of Nuclear Materials*, vol. 318, pp. 207–214, May 2003.

[62] J. J. Kai and R. L. Klueh, “Microstructural analysis of neutron-irradiated martensitic steels,” *Journal of Nuclear Materials*, vol. 230, pp. 116–123, 1996.
[63] M. J. Hackett, J. T. Busby, M. K. Miller, and G. S. Was, “Effects of oversized solutes on radiation-induced segregation in austenitic stainless steels,” *Journal of Nuclear Materials*, vol. 389, no. 2, pp. 265–278, May 2009.
[64] K. Field, J. Bentley, C. Parish, J. T. Busby, and T. R. Allen, “Dependence of Radiation Induced Segregation on Grain Boundary Structure in a 9 wt.% Cr Model Ferritic/Martensitic Steel,” in *The Minerals, Metals, and Materials Society 140th Annual Meeting & Exhibition*, 2011.
[65] E. A. Little, R. Bullough, and M. H. Wood, “On the Swelling Resistance of Ferritic Steel,” *Proceedings of the Royal Society of London: Series A, Mathematical and Physical Sciences*, vol. 372, no. 1751, pp. 565–579, 1980.
[66] J. Marian, B. Wirth, and J. Perlado, “Mechanism of Formation and Growth of <100> Interstitial Loops in Ferritic Materials,” *Physical Review Letters*, vol. 88, no. 25, pp. 1–4, Jun. 2002.
[67] D. S. Gelles, “Microstructural examination of commercial ferritic alloys at 200 dpa,” *Journal of Nuclear Materials*, vol. 233–237, pp. 293–298, 1996.
[68] R. R. Bullough, M. H. Wood, and E. A. Little, “Microstructural explanation for the low swelling of ferritic steels,” in *Effects of Radiation on Materials: Tenth Conference*, 1981, pp. 593–609.
[69] T. Muroga, A. Yamaguchi, and N. Yoshida, “Effects of Radiation on Materials: 14th International Symposium,” in *Volume 1*, 1989, p. 396.
[70] D. S. Gelles, S. Ohnuki, H. Takahashi, H. Matsui, and Y. Kohno, “Electron irradiation experiments in support of fusion materials development,” *Journal of Nuclear Materials*, vol. 191–194, pp. 1336–1341, 1992.
[71] D. Terentyev and L. Malerba, “Interaction of <100> and 1/2<111> dislocation loops with point defects in ferritic alloys,” *Journal of Nuclear Materials*, vol. 377, no. 1, pp. 141–146, Jun. 2008.
[72] Z. Jiao, N. Ham, and G. Was, “Microstructure of helium-implanted and proton-irradiated T91 ferritic/martensitic steel,” *Journal of Nuclear Materials*, vol. 367–370, pp. 440–445, Aug. 2007.
[73] N. Hashimoto and R. L. Klueh, “Microstructural evolution of nickel-doped 9Cr steels irradiated in HFIR,” *Journal of Nuclear Materials*, vol. 305, pp. 153–158, 2002.
[74] K. Asano, Y. Kohno, A. Kohyama, and G. Ayrault, “Microstructural evolution of HT9 under dual-beam charged particle irradiation,” *Journal of Nuclear Materials*, vol. 155–157, pp. 912–915, 1988.
[75] P. Dubuisson, D. Gilbon, and J. L. Seran, “Microstructural evolution of ferritic-martensitic irradiated in the fast breeder reactor Phenix,” *Journal of Nuclear Materials*, vol. 205, pp. 178–189, 1993.
[76] S. A. Maloy et al., “The mechanical properties of 316L/304L stainless steels , Alloy 718 and Mod 9Cr-1Mo after irradiation in a spallation environment,” *Journal of Nuclear Materials*, vol. 296, pp. 119–128, 2001.
[77] C. Deo, C. Tome, R. Lebensohn, and S. Maloy, “Modeling and simulation of irradiation hardening in structural ferritic steels for advanced nuclear reactors,” *Journal of Nuclear Materials*, vol. 377, no. 1, pp. 136–140, Jun. 2008.

[78] R. L. Klueh and J. M. Vitek, "Tensile Behavior of Irradiated 12Cr-1MoVW Steel," *Journal of Nuclear Materials*, vol. 137, pp. 44–50, 1985.
[79] R. L. Klueh and J. M. Vitek, "Elevated-temperature tensile properties of irradiated 9Cr-1MoVNb steel," *Journal of Nuclear Materials*, vol. 132, pp. 27–31, 1985.
[80] Z. Lu, R. G. Faulkner, G. Was, and B. D. Wirth, "Irradiation-induced grain boundary chromium microchemistry in high alloy ferritic steels," *Scripta Materialia*, vol. 58, no. 10, pp. 878–881, May 2008.
[81] J. F. Ziegler, "The Stopping and Range of Ions in Matter (SRIM)," .
[82] *Standard Practice for Neutron Radiation Damge Simulation by Charged-Particle Irradiation*. E 521-96, ASTM International, 2003.
[83] C. C. Herrick, "Vapor Pressure of Liquid Indium," in *Transactions of the Metallurgical Society of AIME - Institute of Metals Division*, 1964.
[84] "Experimental Nuclear Reaction Data," *Brookhaven National Laboratory*. [Online]. Available: http://www.nndc.bnl.gov/exfor7/exfor00.htm.
[85] G. Cliff and G. W. Lorimer, "No Title," *Journal of Microscopy*, vol. 103, p. 203, 1975.
[86] D. B. Williams and C. B. Carter, *Transmission Electron Microscopy*. New York, NY: Plenum Press, 1996.
[87] J. Wiley, *Table of Isotopes*, 8th ed. New York: Wiley-Interscience, 1996.
[88] A. D. Brailsford and R. Bullough, "The rate theory of swelling due to void growth in irradiated metals," *Journal of Nuclear Materials*, vol. 44, pp. 121–135, 1972.
[89] A. D. Brailsford and R. Bullough, "The rate theory of swelling due to void growth in irradiated metals," *Journal of Nuclear Materials*, vol. 44, pp. 121–135, 1972.
[90] "Alloy Data Sheet for T91 Heat #C2269 Slab 7B from Bethlehem Lukens Plate Mill, Plate #A9532."
[91] "Alloy Data Sheet for HCM12A Heat #F114206."
[92] "Alloy Data Sheet for HT9 Heat #9-607."
[93] "Alloy Data Sheet for Fe-9Cr."
[94] Z. Jiao and G. S. Was, "Segregation behavior in proton- and heavy-ion-irradiated ferritic–martensitic alloys," *Acta Materialia*, vol. 59, no. 11, pp. 4467–4481, Jun. 2011.
[95] Z. Jiao, V. Shankar, and G. S. Was, "Phase stability in proton and heavy ion irradiated ferritic–martensitic alloys," *Journal of Nuclear Materials*, vol. 419, no. 1–3, pp. 52–62, Dec. 2011.
[96] R. Klueh, N. Hashimoto, M. Sokolov, P. Maziasz, K. Shiba, and S. Jitsukawa, "Mechanical properties of neutron-irradiated nickel-containing martensitic steels: II. Review and analysis of helium-effects studies," *Journal of Nuclear Materials*, vol. 357, no. 1–3, pp. 169–182, Oct. 2006.
[97] A. Alamo, M. Horsten, X. Averty, E. I. Materna-Morris, M. Rieth, and J. C. Brachet, "Mechanical behavior of reduced-activation and conventional martensitic steels after neutron irradiation in the range 250-450°C," *Journal of Nuclear Materials*, vol. 283–287, pp. 353–357, 2000.
[98] R. L. Klueh and D. J. Alexander, "Embrittlement of Cr-Mo steels after low fluence irradiation in HFIR," *Journal of Nuclear Materials*, vol. 218, pp. 151–160, 1995.
[99] A. C. Hindmarsh, "Ordinary Differential Equation System Solver," *UCID-30001 Rev. 3, Lawrence Livermore National Laboratory*, 1974.

[100] A. C. Hindmarsh, “Linear Multistep Methods for Ordinary Differential Equations: Method Formulations, Stability, and the Methods of Nordiseck and GEAR,” *UCRL-51186 Rev. 1, Lawrence Livermore National Laboratory*, 1972.
[101] A. C. Hindmarsh, “Construction of Mathematical Software, Part III: The Control of Error in the GEAR Package for Ordinary Differential Equations,” *UCID-30050 Part 3, Lawrence Livermore National Laboratory*, 1972.
[102] “SilverFrost FTN95.” [Online]. Available: http://www.silverfrost.com/11/ftn95/overview.aspx. [Accessed: 05-May-2012].
[103] A. L. Nikolaev, V. L. Arbuzov, and A. E. Davletshin, “On the effect of impurities on resistivity recovery, short-range ordering, and defect migration in electron-irradiated concentrated Fe–Cr alloys,” *J. Phys.: Condens. Matter*, vol. 9, p. 4385, 1997.
[104] A. L. Nikolaev, “Stage I of recovery in 5 MeV electron-irradiated iron and iron-chromium alloys: the effect of small cascades, migration of di-interstitials and mixed dumbbells,” *J. Phys.: Condens. Matter*, vol. 11, p. 8633, 1999.
[105] S. Takaki, J. Fuss, H. Kugler, U. Dedek, and H. Schultz, “The resistivity recovery of high purity and carbon doped iron following low temperature electron irradiation,” *Radiation Effects*, vol. 79, pp. 87–122, Jan. 1983.
[106] H. Abe and E. Kuramoto, “Interaction of solutes with irradiation-induced defects of electron-irradiated dilute iron alloys,” *Journal of Nuclear Materials*, vol. 271–272, pp. 209–213, May 1999.
[107] H.-E. Schaefer, K. Maier, M. Weller, D. Herlach, A. Seeger, and J. Diehl, “Vacancy formation in iron investigated by positron annihilation in thermal equilibrium,” *Scripta Metallurgica*, vol. 11, pp. 803–809, 1977.
[108] L. De Schepper et al., “Positron annihilation on pure and carbon-doped α-iron in thermal equilibrium,” *Physical Review B*, vol. 27, no. 9, p. 5257, 1983.
[109] Y. Shirai, “No Title,” in *Annual Meeting of the Physical Society of Japan*, 1987.
[110] Y. Iijima, K. Kimura, and K. Hirano, “Self-diffusion and isotope effect in α-Iron,” *Acta Metallurgica*, vol. 36, no. 10, pp. 2811–2820, 1988.
[111] D. Nguyen-Manh, M. Y. Lavrentiev, and S. L. Dudarev, “The Fe–Cr system: atomistic modelling of thermodynamics and kinetics of phase transformations,” *Comptes Rendus Physique*, vol. 9, pp. 379–388, Apr. 2008.
[112] P. Olsson, C. Domain, and J. Wallenius, “Ab initio study of Cr interactions with point defects in bcc Fe,” *Physical Review B*, vol. 75, no. 1, pp. 1–12, Jan. 2007.
[113] C.-C. Fu, F. Willaime, and P. Ordejón, “Stability and Mobility of Mono- and Di-Interstitials in α-Fe,” *Physical Review Letters*, vol. 92, no. 17, pp. 1–4, Apr. 2004.
[114] D. Terentyev, P. Olsson, T. P. C. Klaver, and L. Malerba, “On the migration and trapping of single self-interstitial atoms in dilute and concentrated Fe–Cr alloys: Atomistic study and comparison with resistivity recovery experiments,” *Computational Materials Science*, vol. 43, no. 4, pp. 1183–1192, Oct. 2008.
[115] P. Olsson, “Ab initio study of interstitial migration in Fe–Cr alloys,” *Journal of Nuclear Materials*, vol. 386–388, pp. 86–89, Apr. 2009.
[116] A. D. LeClaire, “Physical Chemistry,” *Philosophical Magazine*, vol. 21, p. 819, 1970.
[117] A. D. LeClaire, “No Title,” *Journal of Nuclear Materials*, vol. 69, p. 70, 1978.

[118] R. A. Johnson, “Interstitials and vacancies in α Iron,” *Physical Review*, vol. 134, no. 5A, pp. A1329–A1336, 1964.
[119] T. Diaz de la Rubia, N. Soneda, M. J. Caturla, and E. A. Alonso, “Defect production and annealing kinetics in elemental metals and semiconductors,” *Journal of Nuclear Materials*, vol. 251, pp. 13–33, Nov. 1997.
[120] C. M. Walter and N. L. Peterson, “Isotope effect in self-diffusion in iron,” *Physical Review*, vol. 178, no. 3, pp. 922–929, 1969.
[121] D. Graham, “Mass Dependence of Self-Diffusion in Iron,” *Journal of Applied Physics*, vol. 40, no. 6, p. 2386, 1969.
[122] V. Irmer and M. Feller-Kniepmeier, “Isotope effect for self-diffusion in single crystals of α Iron and correlation factor of solute diffusion in α Iron,” *Journal of Applied Physics*, vol. 43, no. 3, pp. 953–957, 1972.
[123] Y. N. Osetsky and A. Serra, “Vacancy and interstitial diffusion in bcc-Fe,” *Defect and Diffusion Forum*, vol. 143–147, pp. 155–160, 1997.
[124] C. Tuijn, H. Bakker, and G. Neumann, “The correlation factor of impurity diffusion in body-centered cubic metals for mixed nearest- and next-nearest-neighbour monovacancy jumps,” *J. Phys.: Condens. Matter*, vol. 4, p. 4801, 1992.
[125] G. Neumann and C. Tuijn, “Impurity diffusion in metals,” in *Diffusion and Defect Data Part B: Solid State Phenomena, Volume 88*, 2002.
[126] S. J. Rothman, L. J. Nowicki, and G. E. Murch, “Self-diffusion in austenitic Fe-Cr-Ni alloys,” *J. Phys. F: Metal Phys.*, vol. 10, pp. 383–398, 1980.
[127] H. Matter, J. Winter, and W. Triftshiiuser, “Phase transformations and vacancy formation energies of transition metals by positron annihilation,” *Applied Physics*, vol. 20, pp. 135–140, 1979.
[128] J. L. Campbell and C. W. Schulte, “Positron trapping and self-diffusion activation energies in Chromium,” *Applied Physics*, vol. 19, pp. 149–152, 1979.
[129] M. A. Tschopp, K. N. Solanki, F. Gao, X. Sun, M. A. Khaleel, and M. F. Horstemeyer, “Probing grain boundary sink strength at the nanoscale: Energetics and length scales of vacancy and interstitial absorption by grain boundaries in α-Fe,” *Physical Review B*, vol. 85, no. 6, pp. 1–21, Feb. 2012.
[130] R. D. Carter, D. L. Damcott, M. Atzmon, G. S. Was, S. M. Bruemmer, and E. A. Kenik, “Quantitative analysis of radiation-induced grain-boundary segregation measurements,” *Journal of Nuclear Materials*, vol. 211, pp. 70–84, 1994.
[131] L. K. Mansur, “Correlation of neutron and heavy-ion damage: II. The predicted temperature sift of swelling with changes in radiation dose rate,” *Journal of Nuclear Materials*, vol. 78, pp. 156–160, 1978.
[132] L. K. Mansur, “Theory of transitions in dose dependence of radiation effects in structural alloys,” *Journal of Nuclear Materials*, vol. 206, no. 2–3, pp. 306–323, Nov. 1993.
[133] R. A. Johnson and N. Q. Lam, “Solute segregation under irradiation,” *Journal of Nuclear Materials*, vol. 69 & 70, pp. 424–433, 1978.
[134] J. Wallenius, P. Olsson, C. Lagerstedt, N. Sandberg, R. Chakarova, and V. Pontikis, “Modeling of chromium precipitation in Fe-Cr alloys,” *Physical Review B*, vol. 69, no. 9, pp. 1–9, Mar. 2004.

[135] D. Farkas, C. G. Schon, M. S. F. De Lima, and H. Goldenstein, “Embedded atom computer simulation of lattice distortion and dislocation core structure and mobility in Fe□Cr alloys,” *Acta Materialia*, vol. 44, no. 1, pp. 409–419, Jan. 1996.
[136] M. Matijasevic and a Almazouzi, “Effect of Cr on the mechanical properties and microstructure of Fe–Cr model alloys after n-irradiation,” *Journal of Nuclear Materials*, vol. 377, no. 1, pp. 147–154, Jun. 2008.
[137] R. Schaeublin, T. Leguey, P. Spätig, N. Baluc, and M. Victoria, “Microstructure and mechanical properties of two ODS ferritic/martensitic steels,” *Journal of Nuclear Materials*, vol. 307–311, pp. 778–782, Dec. 2002.
[138] R. Schaeublin, D. Gelles, and M. Victoria, “Microstructure of irradiated ferritic/martensitic steels in relation to mechanical properties,” *Journal of Nuclear Materials*, vol. 307–311, pp. 197–202, Dec. 2002.
[139] Y. Hosoi, N. Wade, T. Urita, M. Tanino, and H. Komatsu, “Change in microstructure and toughness of ferritic-martensitic stainless steels during long-term aging,” *Journal of Nuclear Materials*, vol. 133–134, pp. 337–342, 1984.
[140] Z. Liu and X. Huang, “Factors that affect activation energy for Li diffusion in LiFePO4: A first-principles investigation,” *Solid State Ionics*, vol. 181, no. 19–20, pp. 907–913, Jul. 2010.
[141] R. L. Fleischer, “Substitutional solutes in AlRu: I. Effects of solute on moduli, lattice parameters, and vacancy production,” *Acta Metallurgica Materialia*, vol. 41, no. 3, pp. 863–869, 1993.
[142] R. Fleischer, “Substitutional solutes in AlCo: I. Effects of solute on moduli, lattice parameters, and vacancy production,” *Journal of Materials Research*, vol. 8, no. 1, pp. 49–58, 1993.
[143] J. P. Wharry, Z. Jiao, V. Shankar, J. T. Busby, and G. S. Was, “Radiation-induced segregation and phase stability in ferritic–martensitic alloy T91,” *Journal of Nuclear Materials*, vol. 417, no. 1–3, pp. 140–144, Oct. 2011.
[144] C. R. Hubbard, H. E. Swanson, and F. A. Mauer, “A silicon powder diffraction standard reference material,” *Journal of Applied Crystallography*, vol. 8, pp. 45–48, 1975.
[145] A. Taylor, “Lattice parameters of binary nickel-cobalt alloys,” *Journal of the Institute of Metals*, vol. 77, pp. 585–594, 1950.
[146] M. E. Straumanis and L. S. Yu, “Lattice parameters, densities, expansion coefficients and perfection of structure of Cu and of Cu-In α phase,” *Acta Crystallographica, Section A (Crystal Physics, Diffraction, Theoretical and General Crystallography)*, vol. A25, no. 6, pp. 676–682, 1969.
[147] R. G. Ross and W. Hume-Rothery, “High temperature x-ray metallography, I. A new Debye-Scherrer camera for use at very high temperatures, II. A new parafocusing camera, III. Applications to the study of chromium, hafnium, molybdenum, rhodium, ruthenium, and tungsten,” *Journal of the Less-Common Metals*, vol. 5, no. 2, pp. 258–270, 1963.
[148] N. Schmitz-Pranghe and R. Kohlhaas, “X-ray diffraction investigation of liquid iron, cobalt and nickel,” *Zeitschrift fur Naturforschung A (Astrophysik, Physik und Physikalische Chemie)*, vol. 25, no. 11, p. 1752, 1970.